

## Electronic Supplementary Information

### The influence of the terminal acceptor and oligomer length on the photovoltaic properties of A-D-A small molecule donors

Fernando G. Guijarro,<sup>a</sup> Prateek Malhotra,<sup>b</sup> Gaurav Gupta,<sup>b</sup> Ruben Caballero,<sup>a</sup> Pilar de la Cruz,<sup>a</sup> Rahul Singhal,<sup>c</sup> Ganesh D. Sharma<sup>\*b</sup> and Fernando Langa<sup>\*a</sup>.

<sup>a</sup>*Universidad de Castilla-La Mancha, Institute of Nanoscience, Nanotechnology and Molecular Materials (INAMOL), Campus de la Fábrica de Armas, 45071-Toledo, Spain*

<sup>b</sup>*Department of Physics, The LNM Institute of Information Technology, Deemed University, Jamdoli, Jaipur (Raj.) 302031, India*

<sup>c</sup>*Department of Physics, MNIT, JLN Marg, Jaipur 302017, India*

### Contents

<b>1. General Remarks .....</b>	S2
<b>2. Synthesis of FG1-4 .....</b>	S4
<b>3. <math>^1\text{H}</math> NMR, <math>^{13}\text{C}</math> NMR, <math>^{13}\text{C}</math> NMR DEPT135, FT-IR and MALDI-TOF spectra .....</b>	S6
<b>4. Thermogravimetric Analysis (TGA) and Differential Scanning Calorimetry (DSC) of compounds FG1-4 .....</b>	S18
<b>5. Absorption spectrum in solution .....</b>	S20
<b>6. Electrochemical Studies .....</b>	S21
<b>7. Theoretical calculations.....</b>	S23

## 1. General Remarks

**Experimental Conditions.** Solvents and chemicals were purchased from Aldrich Chemicals (Milwaukee, WI). Anhydrous solvents, where indicated, were dried using a Pure-Sov 400 or using standard techniques. Chromatographic purifications were performed using silica gel 60 VWR (particle size 0.040-0.063 mm). Analytical thin-layer chromatography was performed using Merck TLC silica gel 60 F254. <sup>1</sup>H NMR spectra were recorded as solutions in a partial deuterated solvent on a Brüker-Topspin AV 400 instrument. Chemical shifts are given as  $\delta$  values. <sup>1</sup>H NMR chemical shifts are reported relative to residual non deuterated solvent peaks. <sup>13</sup>C NMR chemical shifts are reported relative to the deuterated solvent peak. FT-IR spectra were recorded in an AVATAR 370 FT-IR Thermo Nicolet spectrometer. Mass spectra (MALDI-TOF) were recorded on a VOYAGER DTM STR mass spectrometer using dithranol as matrix. UV/Vis spectra were recorded on a Shimadzu UV-VIS-NIR spectrophotometer UV-3600 in quartz cuvettes with a path length of 1 cm. Fluorescence measurements were carried out on Cary Eclipse fluorescence spectrophotometer.

**Electrochemical Measurements.** Cyclic and Oyster-Young Square wave voltammetry were performed in a  $\mu$ AUTOLAB Type II potentiostat, using 0.1M solution of Tetrabutylammonium perchlorate in 1,2-dichlorobenzene:acetonitrile 4:1 as a supporting electrolyte. Solutions were deoxygenated by bubbling argon through prior to each measurement which was run under an argon atmosphere. Experiments were carried out in a one-compartment cell equipped with a glassy carbon electrode, a platinum wire counter electrode and an Ag/AgNO<sub>3</sub> as pseudo reference electrode. All Potentials were checked against the ferrocene/ferrocenium couple (Fc/Fc<sup>+</sup>) after each experiment. Melting points are recorded in Gallenkamp melting point apparatus and are uncorrected. Thermogravimetric analyses were performed using a TGA/DSC Linea Excellent instrument by Mettler-Toledo and collected under inert atmosphere of nitrogen with a scan rate of 10 °C min<sup>-1</sup>. The weight changes were recorded as a function of temperature.

**Computational Details:** Theoretical calculations were carried out within the density functional theory (DFT) framework by using the Gaussian 09,<sup>1</sup> applying density functional theory at the B3LYP level. The basis set of 6-31G\* was used in the calculations (Supercomputation Service of UCLM).

---

<sup>1</sup> Gaussian 09, Revision A.1, M. J. Frisch, G. W. Trucks, H. B. Schlegel, G. E. Scuseria, M. A. Robb, J. R. Cheeseman, G. Scalmani, V. Barone, B. Mennucci, G. A. Petersson, H. Nakatsuji, M. Caricato, X. Li, H. P. Hratchian, A. F. Izmaylov, J. Bloino, G. Zheng, J. L. Sonnenberg, M. Hada, M. Ehara, K. Toyota, R. Fukuda, J. Hasegawa, M. Ishida, T. Nakajima, Y. Honda, O. Kitao, H. Nakai, T. Vreven, J. A. Montgomery, Jr., J. E. Peralta, F. Ogliaro, M. Bearpark, J. J. Heyd, E. Brothers, K. N. Kudin, V. N. Staroverov, R. Kobayashi, J. Normand, K. Raghavachari, A. Rendell, J. C. Burant, S. S. Iyengar, J. Tomasi, M. Cossi, N. Rega, J. M. Millam, M. Klene, J. E. Knox, J. B. Cross, V. Bakken, C. Adamo, J. Jaramillo, R. Gomperts, R. E. Stratmann, O. Yazyev, A. J. Austin, R. Cammi, C. Pomelli, J. W. Ochterski, R. L. Martin, K. Morokuma, V. G. Zakrzewski, G. A. Voth, P. Salvador, J. J. Dannenberg, S. Dapprich, A. D. Daniels, O. Farkas, J. B. Foresman, J. V. Ortiz, J. Cioslowski, and D. J. Fox, Gaussian, Inc., Wallingford CT, 2009.

**Preparation of devices.** We have fabricated all the OSCs using the conventional structure having ITO/PEDOT:PSS/active layer/PFN/Al. The indium tin oxide coated glass substrates were cleaned using ultrasonic cleaner in detergent, deionized water, acetone and isopropanol successively for 20 min each and then dried into the vacuum oven at temperature of 40° C. PEDOT:PSS was spin coated onto the top of ITO substrates at 3500 rpm and then annealed at 110 C for 10 min. The blend donor (**FG1-4**) and PC<sub>71</sub>BM with different weight ratios (total concentration of 16 mg/mL) were dissolved into benzonitrile solution and then thin film of active layer was spin cast at 3000 rpm on to the top of PEDOT:PSS film and dried at room temperature. PFN was dissolved on methanol at the concentration of 0.5 mg/mL and spin cast at 2000 rpm for 30s on the top of active layer. SVA treatment was carried out in the presence of THF environment for 40s. After that aluminum (Al) was thermally evaporated at a vacuum of  $\leq 1.0 \times 10^{-5}$  Pa. The effective area of all the devices is 4x4 mm<sup>2</sup>. Current -voltage (J-V) measurements were carried out using a Keithley source meter unit under AM 1.5 G (100 mW/cm<sup>2</sup>) by a solar simulator. Incident photon to current conversion efficiency spectra were measured using Bentham PVE 300 EQE system. The J-V under illumination and IPCE spectra of the devices were recorded using a mask of aperture are of 6x6 mm<sup>2</sup>. The hole-only (ITO/PEDOT:PSS/active layer/Au and electron-only (ITO/Al/active layer/Al) devices were prepared to measure the hole and electron mobility, respectively employing the optimized active layer.

## 2. Synthesis of FG1-4

### General procedure for Knoevenagel reaction.

Under argon atmosphere, piperidine was added over a solution of the corresponding bisaldehyde (**1** or **2**) and rhodanine derivative (**3a** or **3b**) in anhydrous CHCl<sub>3</sub>. The resulting solution was heated to reflux for the indicated time. After this, water was added, and the organic phase was extracted with chloroform. The organic phase was dried over anhydrous MgSO<sub>4</sub>, filtered and evaporated to dryness. The crude was purified by chromatographic techniques and eventually recrystallized with the specified solvents to obtain **FG1-4** as solids.

**Synthesis of FG1.** Prepared accordingly to the general procedure for Knoevenagel reaction, using bisaldehyde **1**<sup>2</sup> (60 mg, 0.077 mmol, 1 eq), 3-ethylrhodanine **3a** (50 mg, 0.308 mmol, 4 eq), piperidine (50 µl) and anhydrous CHCl<sub>3</sub> (5 mL). Reaction time: 21 hours. Purification: Column chromatography (Silica gel, Hexane:CHCl<sub>3</sub> 50:50) and then washed with methanol to obtain **FG1** as an orange solid (79 mg, 96%). M.P.: 229-230 °C. <sup>1</sup>H-NMR (400 MHz, CDCl<sub>3</sub>) δ/ppm: 7.86 (s, 2H), 7.20 (s, 2H), 7.07 (s, 2H), 6.94 (s, 2H), 4.19 (q, 4H, <sup>3</sup>J= 7.0Hz), 1.86 (m, 8H), 1.29 (m, 9H), 1.16 (m, 22H), 0.96 (m, 7H), 0.82 (t, 12H, <sup>3</sup>J= 7.0Hz). <sup>13</sup>C-NMR (100 MHz, CDCl<sub>3</sub>) δ/ppm: 191.6, 167.3, 161.9, 159.7, 147.0, 146.4, 138.8, 135.4, 127.9, 126.4, 121.8, 121.0, 117.5, 54.1, 39.9, 37.8, 31.6, 29.6, 24.6, 22.6, 14.1, 12.3. FT-IR (KBr) v/cm<sup>-1</sup>: 2924, 2854, 1697, 1577, 1481, 1412, 1381, 1319, 1234, 1126, 1103, 887, 733, 509. MS (m/z) (MALDI-TOF): calculated for C<sub>56</sub>H<sub>70</sub>N<sub>2</sub>O<sub>2</sub>S<sub>8</sub> 1058.32; found: 1059.00 (M+H). UV-Vis (CH<sub>2</sub>Cl<sub>2</sub>) λ<sub>max</sub>/nm (log ε): 642 nm (4.98).

**Synthesis of FG2.** Prepared accordingly to the general procedure for Knoevenagel reaction, using bisaldehyde **2**<sup>2</sup> (87 mg, 0.076 mmol, 1 eq), 3-ethylrhodanine **3a** (49 mg, 0.304 mmol, 4 eq), piperidine (50 µl) and anhydrous CHCl<sub>3</sub> (5 mL). Reaction time: 14 hours. Purification: Column chromatography (Silica gel, Hexane:CHCl<sub>3</sub> 25:75) and recrystallization in a mixture of CH<sub>2</sub>Cl<sub>2</sub> Acetonitrile to obtain **FG2** as an orange solid. (80 mg, 74%). M.P.: 261-262 °C. <sup>1</sup>H-NMR (400 MHz, CDCl<sub>3</sub>) δ/ppm: 7.87 (s, 2H), 7.20 (s, 2H), 7.08 (d, 2H, <sup>3</sup>J= 15.6Hz), 6.98 (d, 2H, <sup>3</sup>J= 15.6Hz), 6.92 (s, 2H), 6.89 (s, 2H), 4.20 (q, 4H, <sup>3</sup>J= 7.1Hz), 1.86 (m, 12H), 1.30 (t, 6H, <sup>3</sup>J= 7.1Hz), 1.16 (m, 37H), 0.96 (m, 11H), 0.82 (m, 18H). <sup>13</sup>C-NMR (100 MHz, CDCl<sub>3</sub>) δ/ppm: 191.6, 167.3, 162.1, 159.5, 159.4, 147.8, 146.8, 143.7, 138.4, 136.7, 134.6, 127.9, 126.5, 122.5, 121.3, 120.2, 119.9, 117.0, 54.0, 53.8, 39.9, 37.8, 31.7, 31.6, 29.7, 29.6, 24.6, 22.7, 22.6, 14.1, 14.0, 12.3. FT-IR (KBr) v/cm<sup>-1</sup>: 2926, 2856, 1697, 1574, 1481, 1411, 1380, 1319, 1234, 1126, 1102, 886, 731, 515. MS (m/z) (MALDI-TOF): calculated for C<sub>79</sub>H<sub>100</sub>N<sub>2</sub>O<sub>2</sub>S<sub>10</sub> 1428.50; found: 1429.07 (M+H). UV-Vis (CH<sub>2</sub>Cl<sub>2</sub>) λ<sub>max</sub>/nm (log ε): 644 nm (5.03).

<sup>2</sup> Burrezo, P. M.; Domínguez, R.; Zafra, J. L.; Pappenfus, T. M.; de la Cruz, P.; Welte, L.; Janzen, D. E.; López Navarrete, J. T.; Langa, F.; Casado, J. *Chem. Sci.* **2017**, 8, 8106.

**Synthesis of FG3.** Prepared accordingly to the general procedure for Knoevenagel reaction, using bisaldehyde **1**<sup>2</sup> (102 mg, 0.132 mmol, 1 eq), 2-(1,1-dicyanomethylene)-3-ethylrhodanine **3b**<sup>3</sup> (102 mg, 0.528 mmol, 4 eq), piperidine (50  $\mu$ l) and anhydrous CHCl<sub>3</sub> (8 mL). Reaction time: 4 hours. Purification: Column chromatography (Silica gel, Hexane:CHCl<sub>3</sub> 25:75) and recrystallization in a mixture of CH<sub>2</sub>Cl<sub>2</sub> Acetonitrile to obtain **FG3** as a greenish-brown solid (75 mg, 50%). M.P.: 269–270 °C. <sup>1</sup>H-NMR (400 MHz, CD<sub>2</sub>Cl<sub>2</sub>)  $\delta$ /ppm: 8.07 (s, 2H), 7.32 (s, 2H), 7.13 (s, 2H), 7.01 (s, 2H), 4.28 (q, 4H, <sup>3</sup>J= 7.1Hz), 1.91 (m, 8H), 1.38 (t, 6H, <sup>3</sup>J= 7.1Hz), 1.16 (m, 24H), 0.97 (m, 8H), 0.81 (t, 12H, <sup>3</sup>J= 7.1Hz). <sup>13</sup>C-NMR (100 MHz, CD<sub>2</sub>Cl<sub>2</sub>)  $\delta$ /ppm: 166.4, 165.8, 163.4, 160.6, 148.4, 147.9, 138.3, 135.9, 130.1, 129.5, 122.5, 121.9, 114.3, 113.2, 110.9, 55.2, 54.8, 41.1, 38.2, 32.1, 30.1, 25.1, 23.1, 14.5, 14.3. FT-IR (KBr)  $\nu$ /cm<sup>-1</sup>: 2926, 2856, 2215, 1713, 1574, 1535, 1450, 1411, 1373, 1326, 1203, 1110, 894, 731, 538, 507. MS (m/z) (MALDI-TOF): calculated for C<sub>62</sub>H<sub>70</sub>N<sub>6</sub>O<sub>2</sub>S<sub>6</sub> 1122.39; found: 1122.88 (M+H). UV-Vis (CH<sub>2</sub>Cl<sub>2</sub>)  $\lambda_{\text{max}}$ /nm (log  $\epsilon$ ): 664 nm (5.00).

**Synthesis of FG4.** Prepared accordingly to the general procedure for Knoevenagel reaction, using bisaldehyde **2**<sup>2</sup> (83 mg, 0.073 mmol, 1 eq), 2-(1,1-dicyanomethylene)-3-ethylrhodanine **3b**<sup>3</sup> (82 mg, 0.511 mmol, 7 eq), piperidine (50  $\mu$ l) and anhydrous CHCl<sub>3</sub> (5 mL). Reaction time: 24 hours. Purification: Column chromatography (Silica gel, Hexane:CHCl<sub>3</sub> 15:85) and recrystallization in a mixture of CH<sub>2</sub>Cl<sub>2</sub> Acetonitrile to obtain **FG4** as a brown solid. (71 mg, 65%). M.P.: 286–287 °C. <sup>1</sup>H-NMR (400 MHz, CD<sub>2</sub>Cl<sub>2</sub>)  $\delta$ /ppm: 8.01 (s, 2H), 7.32 (s, 2H), 7.08 (d, 2H, <sup>3</sup>J= 15.6Hz), 6.97 (d, 2H, <sup>3</sup>J= 15.6Hz), 6.96 (s, 2H), 4.27 (q, 4H, <sup>3</sup>J= 7.1Hz), 1.92 (m, 12H), 1.39 (t, 6H, <sup>3</sup>J= 7.1Hz), 1.19 (m, 36H), 1.01 (m, 12H), 0.82 (m, 18H). <sup>13</sup>C-NMR (100 MHz, CD<sub>2</sub>Cl<sub>2</sub>)  $\delta$ /ppm: 166.3, 165.8, 163.6, 160.3, 160.1, 149.4, 148.4, 144.5, 137.9, 137.4, 135.0, 130.1, 129.8, 123.3, 122.2, 121.0, 120.2, 114.3, 113.3, 110.3, 55.0, 54.8, 41.0, 38.3, 32.3, 32.2, 30.3, 30.1, 25.2, 23.2, 23.1, 14.5, 14.4, 14.3. FT-IR (KBr)  $\nu$ /cm<sup>-1</sup>: 2926, 2856, 2215, 1713, 1574, 1535, 1458, 1373, 1326, 1203, 1110, 925, 894, 731, 538, 507. MS (m/z) (MALDI-TOF): calculated for C<sub>85</sub>H<sub>100</sub>N<sub>6</sub>O<sub>2</sub>S<sub>8</sub> 1492.57; found: 1493.16 (M+H). UV-Vis (CH<sub>2</sub>Cl<sub>2</sub>)  $\lambda_{\text{max}}$ /nm (log  $\epsilon$ ): 676 nm (5.06).

---

<sup>3</sup> Zhang, Q.; Kan, B.; Liu, F.; Long, G.; Wan, X.; Chen, X.; Zuo, Y.; Ni, W.; Zhang, H.; Li, M.; Hu, Z.; Huang, F.; Cao, Y.; Liang, Z.; Zhang, M.; Russell, T. P.; Chen, Y. *Nat. Photonics*, **2014**, 9, 35.

**3.  $^1\text{H}$  NMR,  $^{13}\text{C}$  NMR,  $^{13}\text{C}$  NMR DEPT135, FT-IR and MALDI-TOF spectra**

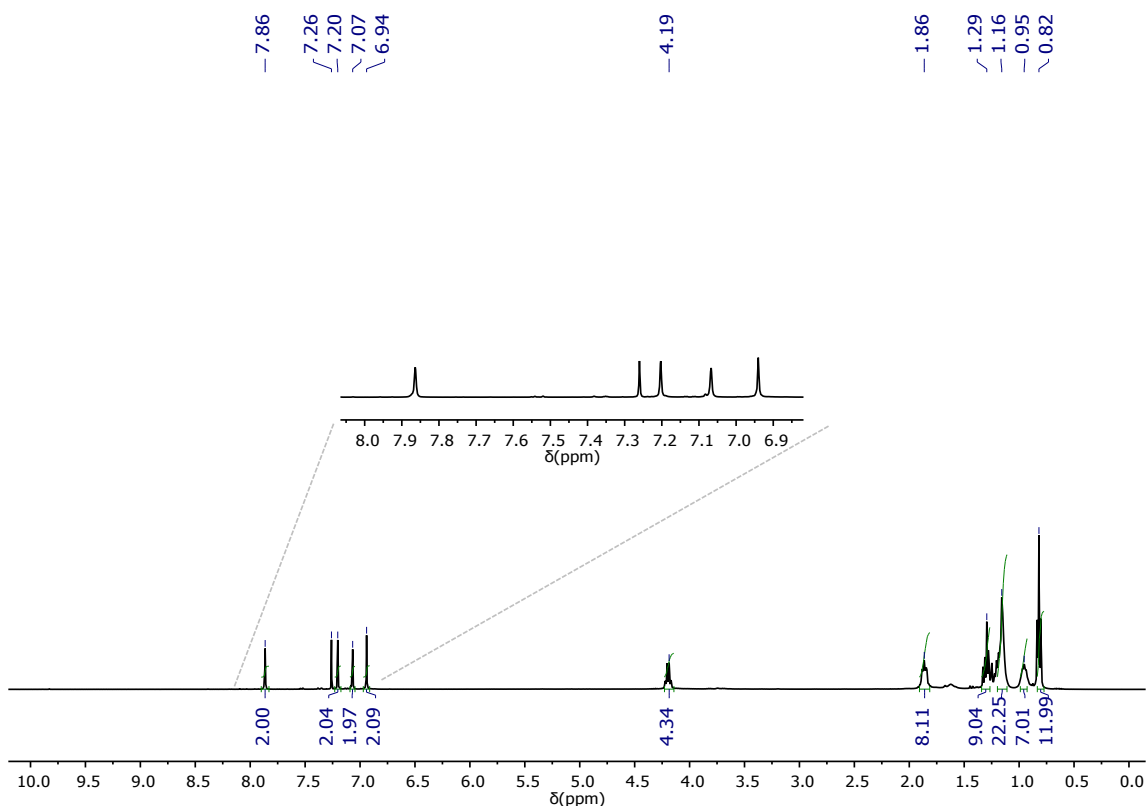


**Figure S1.**  $^1\text{H}$  NMR (400 MHz,  $\text{CDCl}_3$ ) spectrum of compound **FG1**

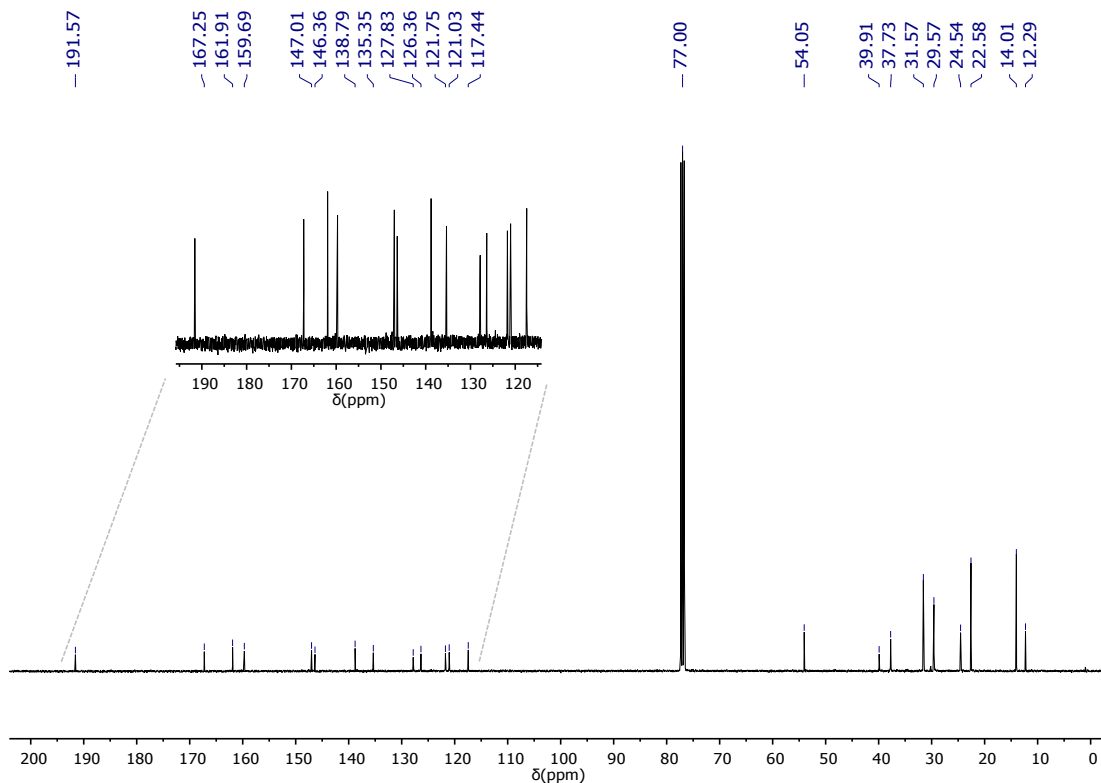


**Figure S2.**  $^{13}\text{C}$  NMR (100 MHz,  $\text{CDCl}_3$ ) spectrum of compound **FG1**

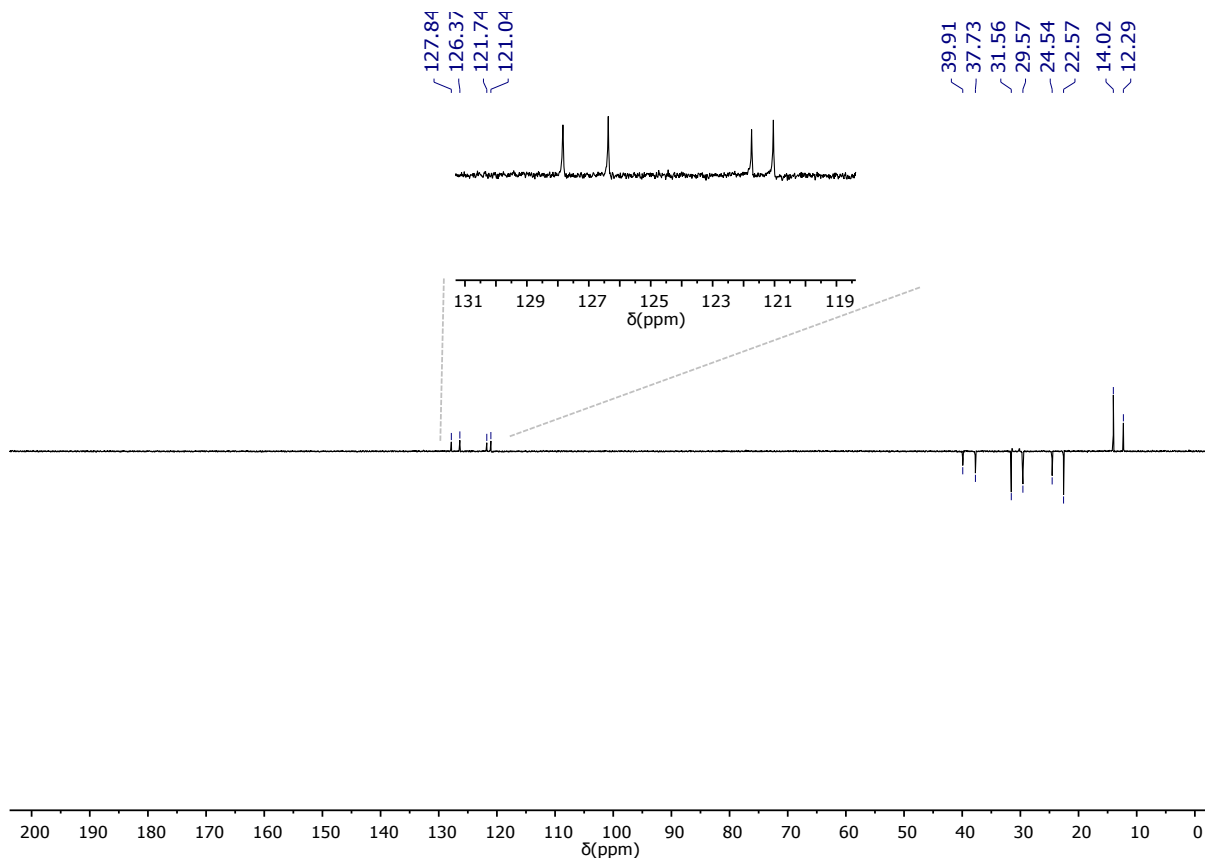


**Figure S3.**  $^{13}\text{C}$  NMR DEPT135 (100 MHz,  $\text{CDCl}_3$ ) spectrum of compound **FG1**

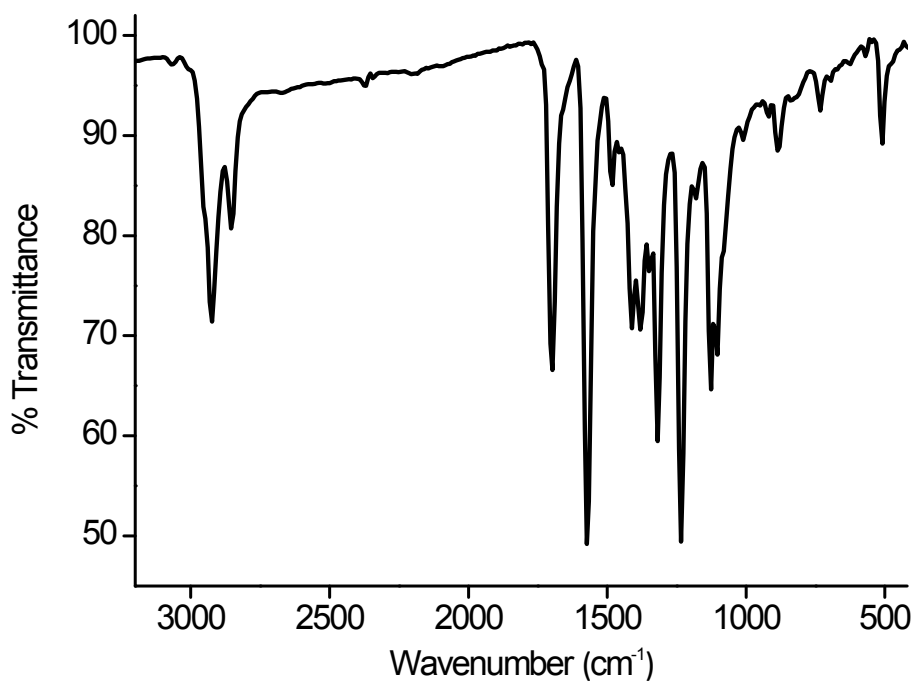


**Figure S4.** FT-IR (KBr) spectrum of compound **FG1**

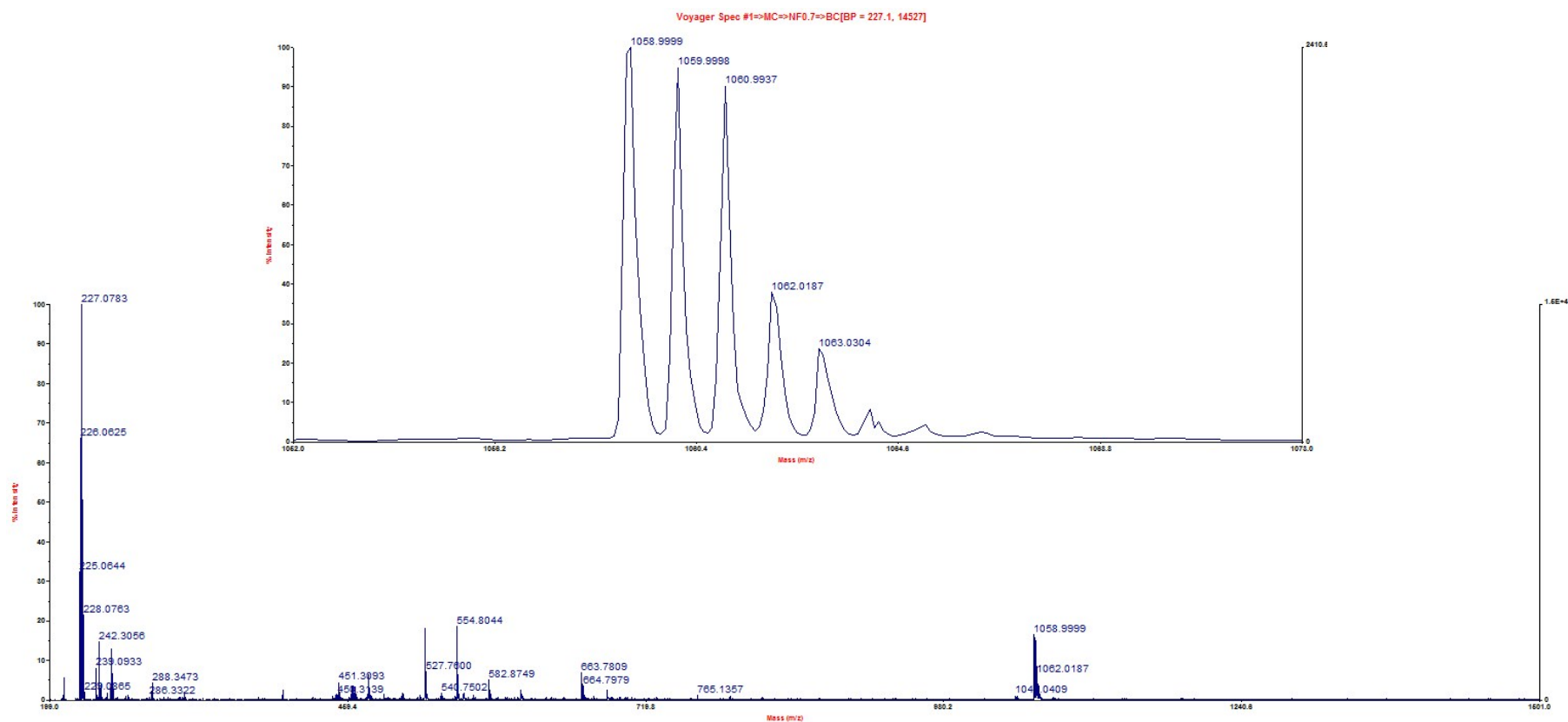


**Figure S5.** MS (MALDI-TOF) spectrum of compound **FG1** (Matrix: Dithranol).

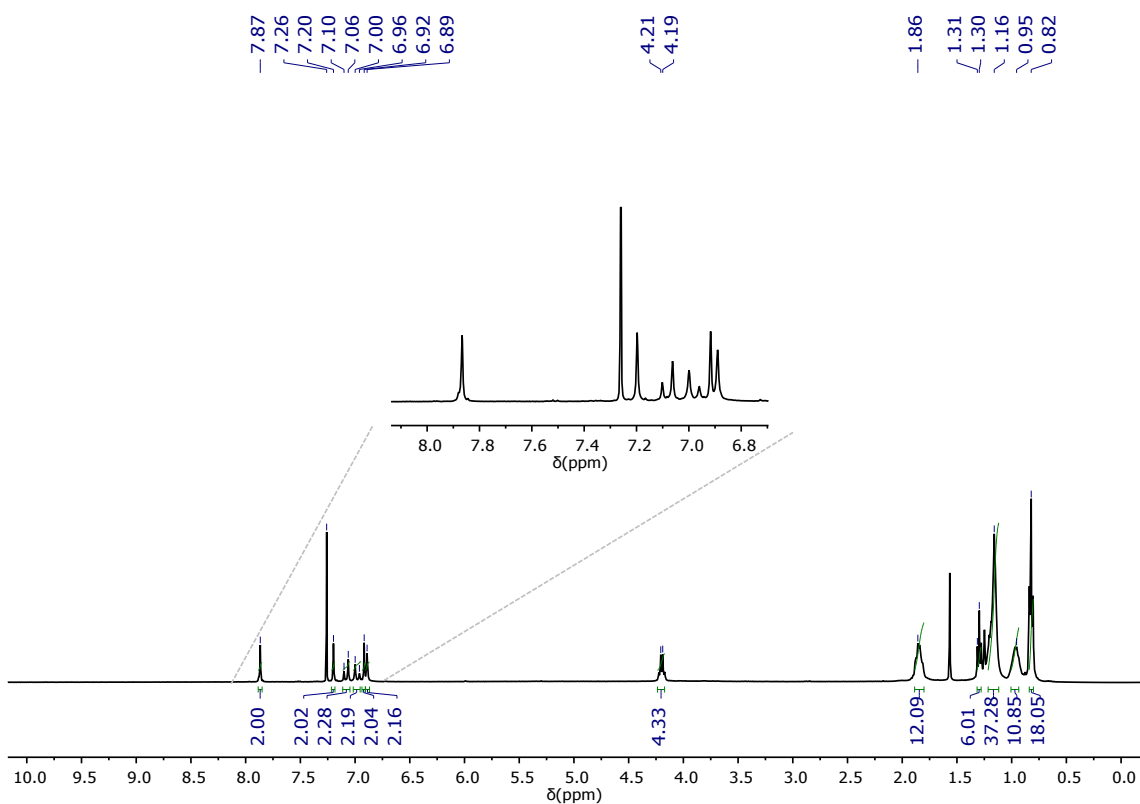


**Figure S6.**  $^1\text{H}$  NMR (400 MHz,  $\text{CDCl}_3$ ) spectrum of compound **FG2**

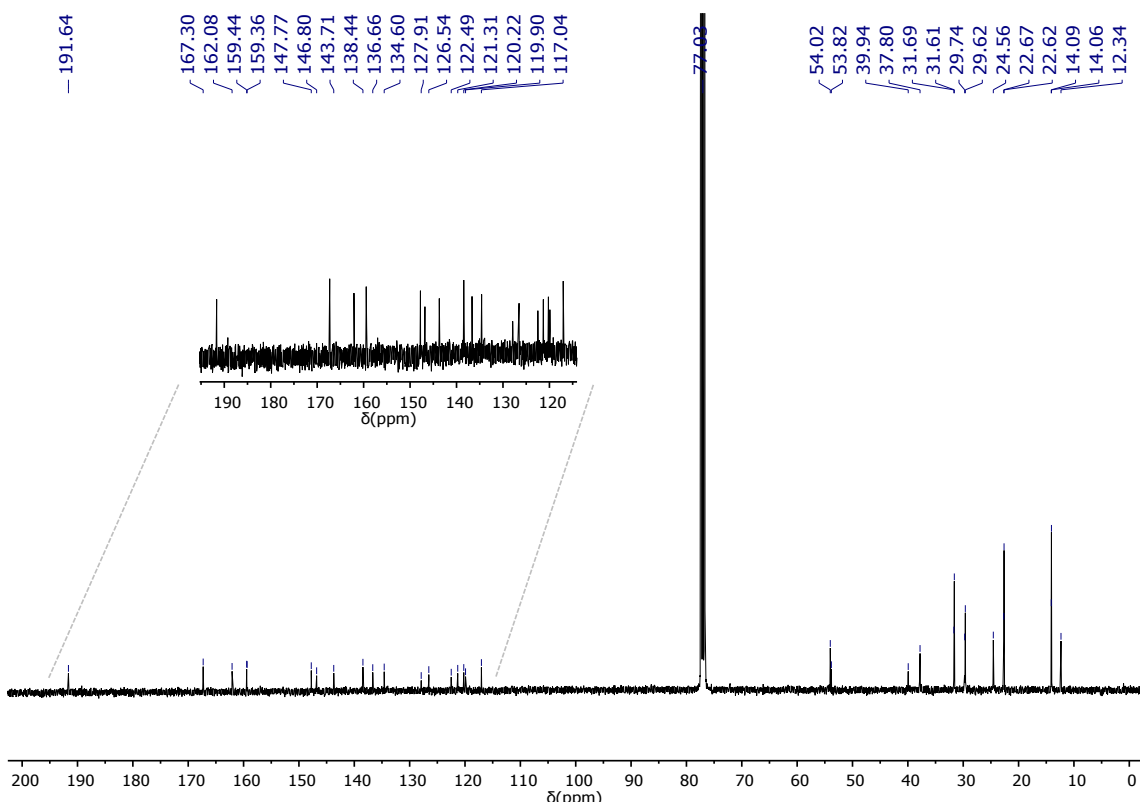


**Figure S7.**  $^{13}\text{C}$  NMR (100 MHz,  $\text{CDCl}_3$ ) spectrum of compound **FG2**

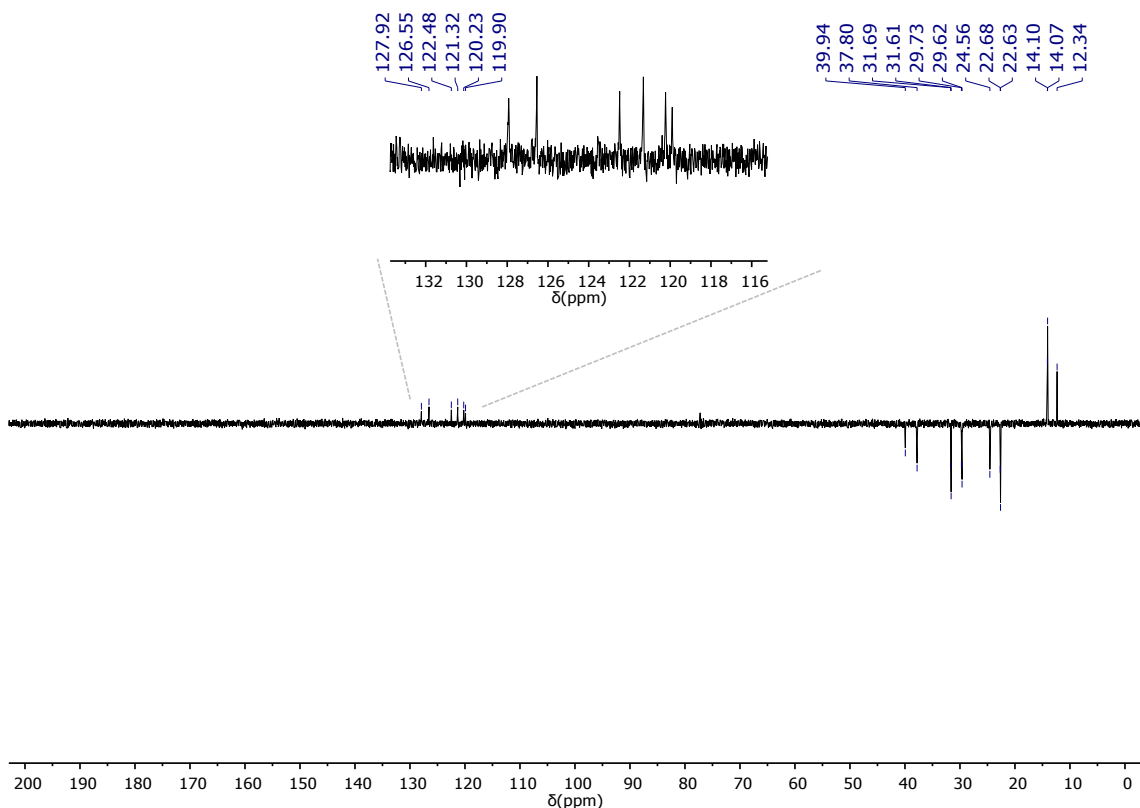


**Figure S8.** <sup>13</sup>C NMR DEPT135 (100 MHz, CDCl<sub>3</sub>) spectrum of compound **FG2**

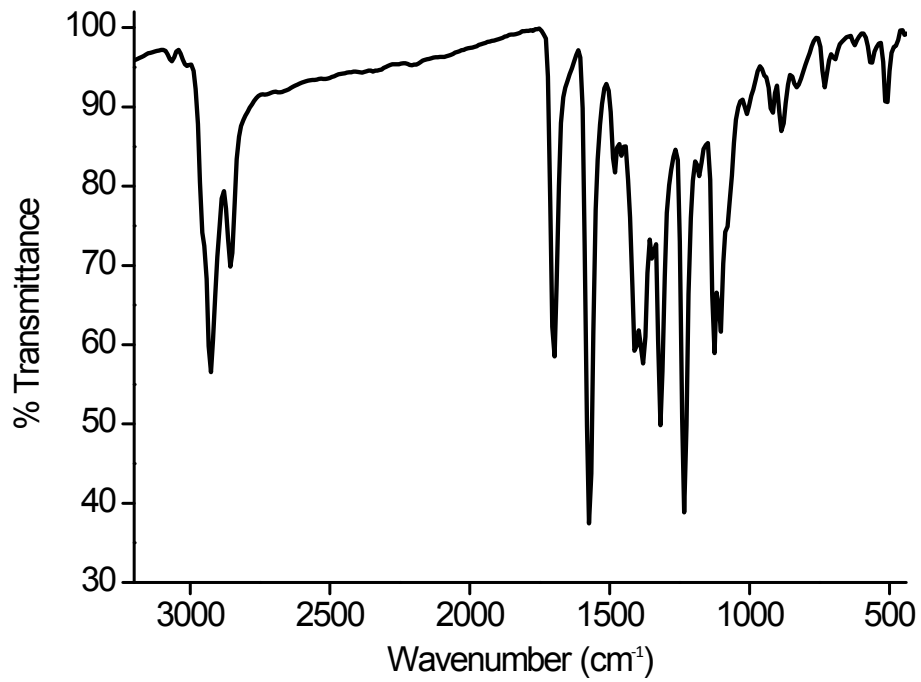


**Figure S9.** FT-IR (KBr) spectrum of compound **FG2**

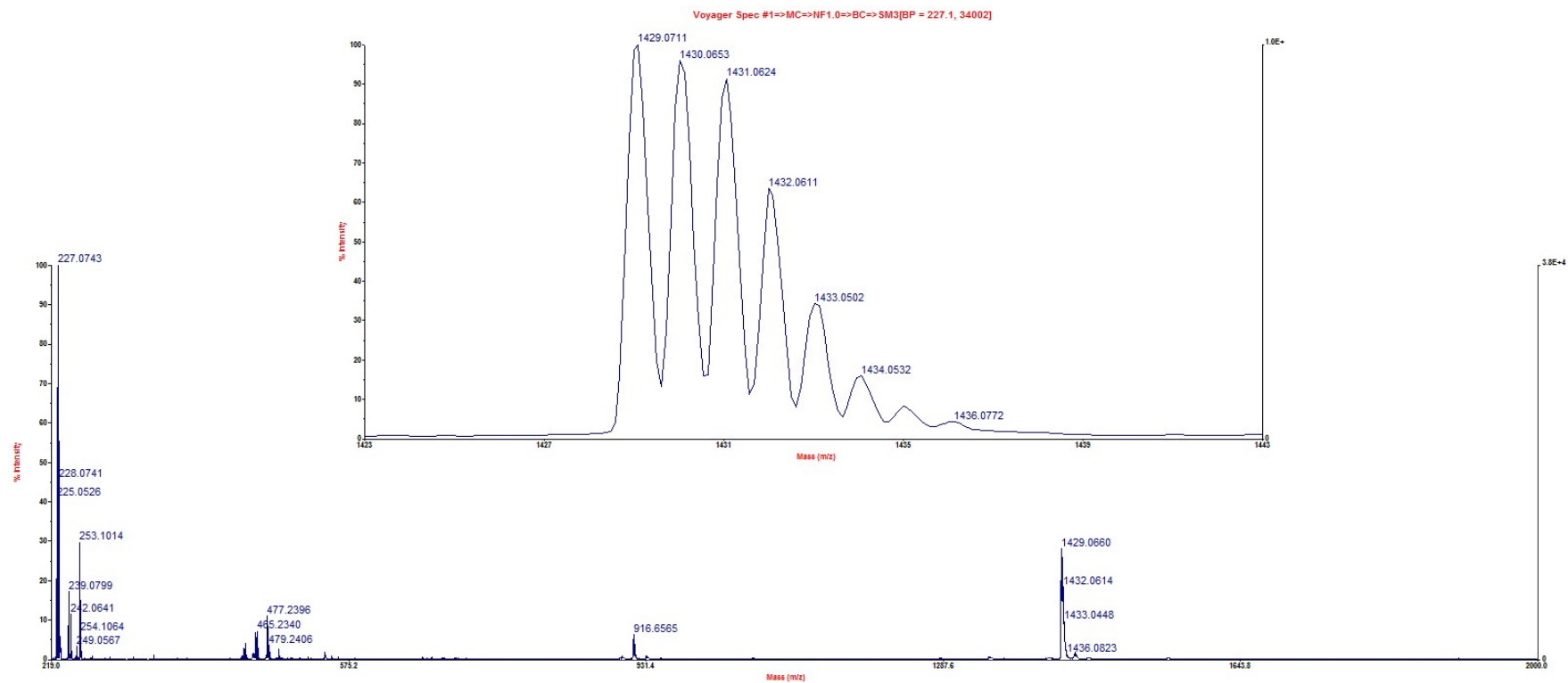


**Figure S10.** MS (MALDI-TOF) spectrum of compound **FG2** (Matrix: Dithranol).

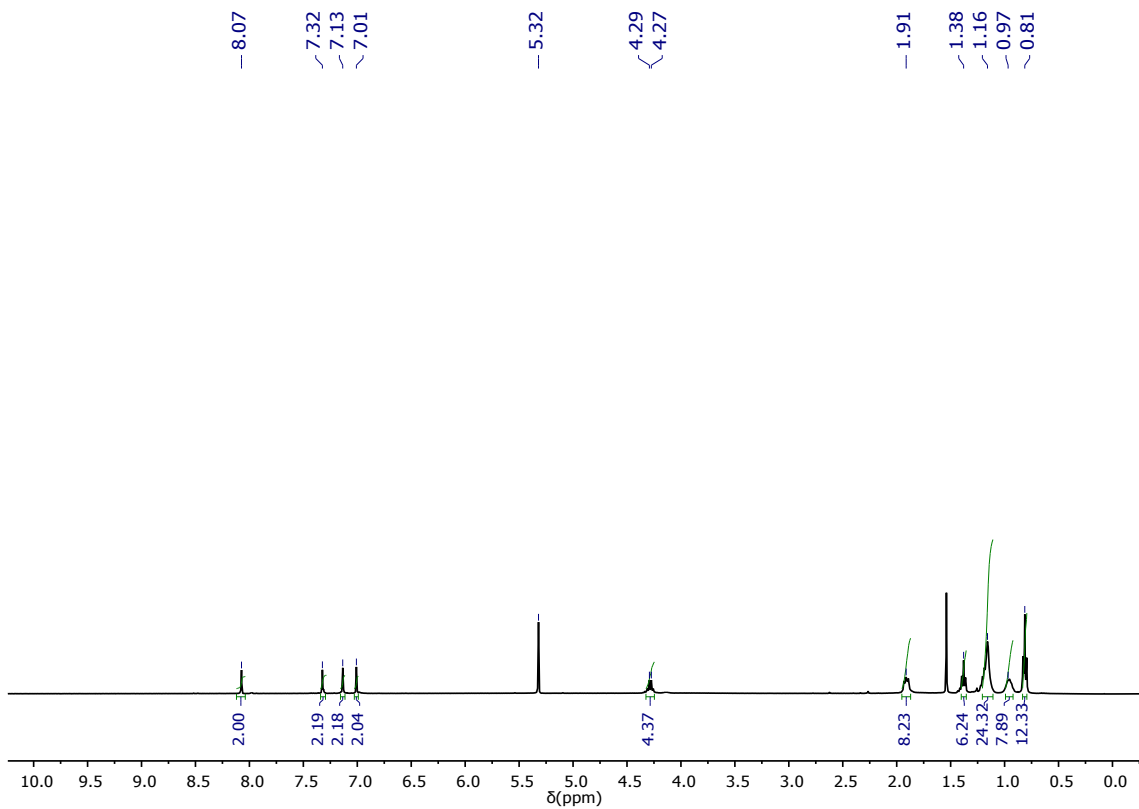


**Figure S11.**  $^1\text{H}$  NMR (400 MHz,  $\text{CD}_2\text{Cl}_2$ ) spectrum of compound **FG3**

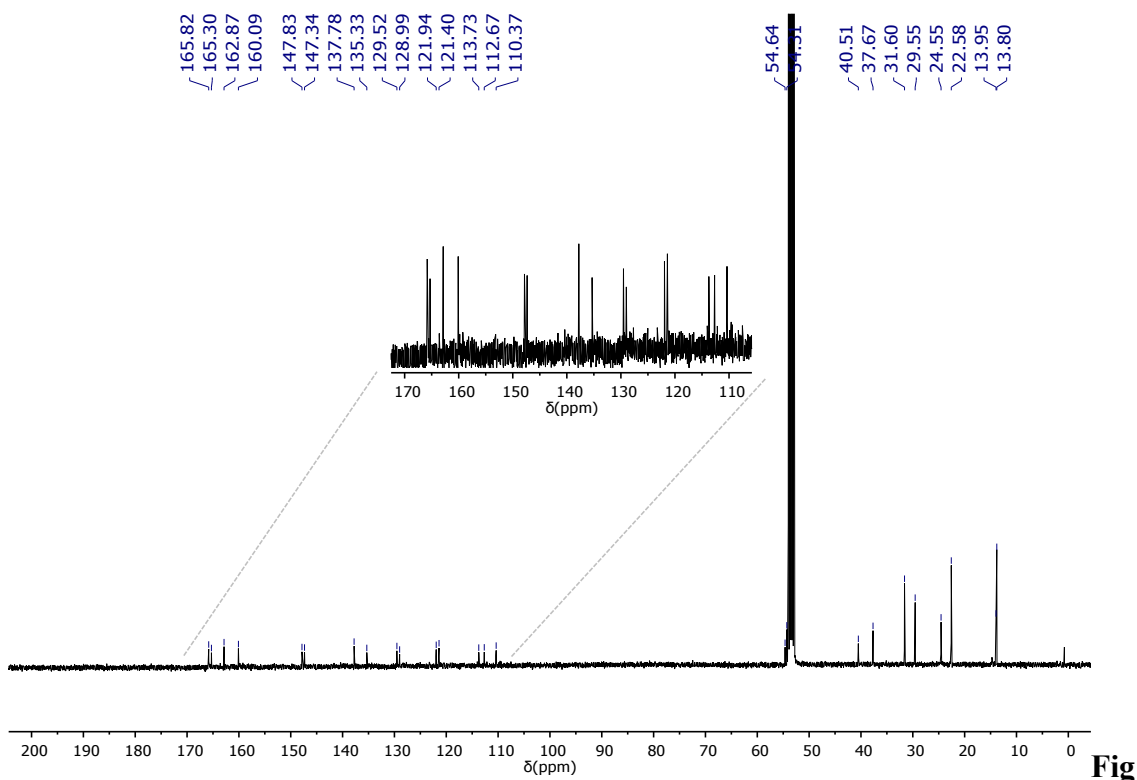


**Figure S12.**  $^{13}\text{C}$  NMR (100 MHz,  $\text{CD}_2\text{Cl}_2$ ) spectrum of compound **FG3**

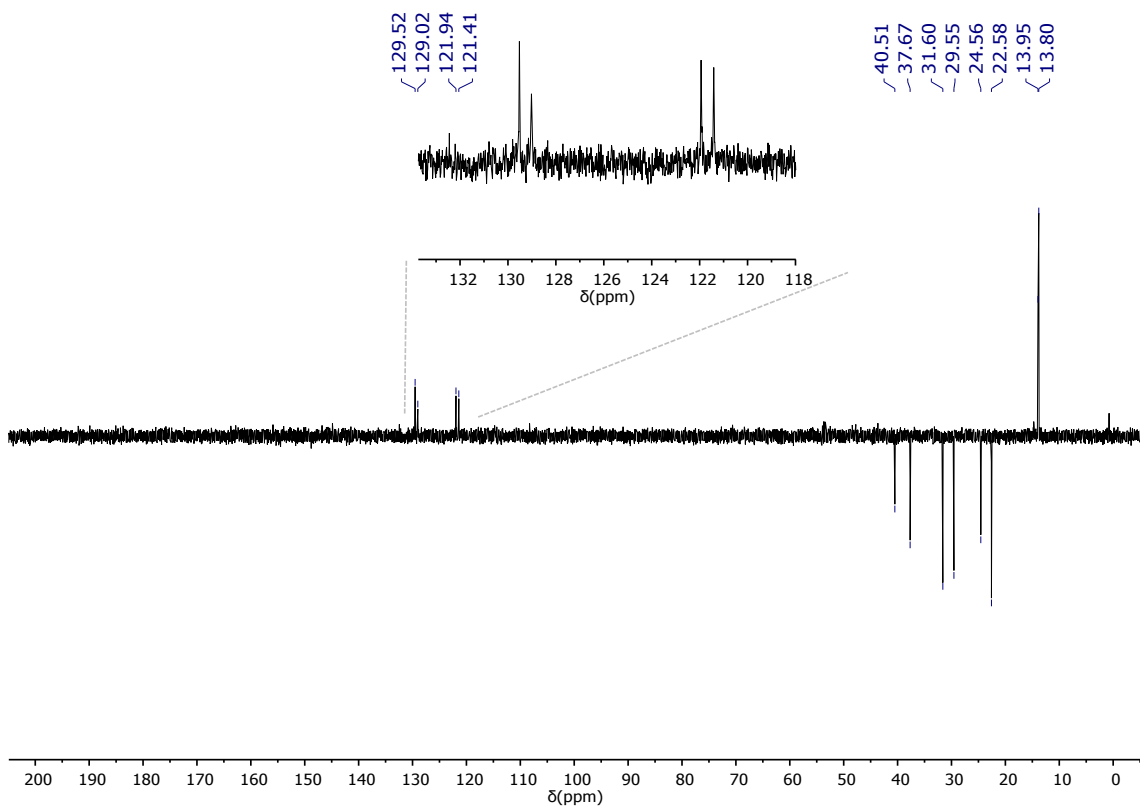


**Figure S13.**  $^{13}\text{C}$  NMR DEPT135 (100 MHz,  $\text{CD}_2\text{Cl}_2$ ) spectrum of compound **FG3**

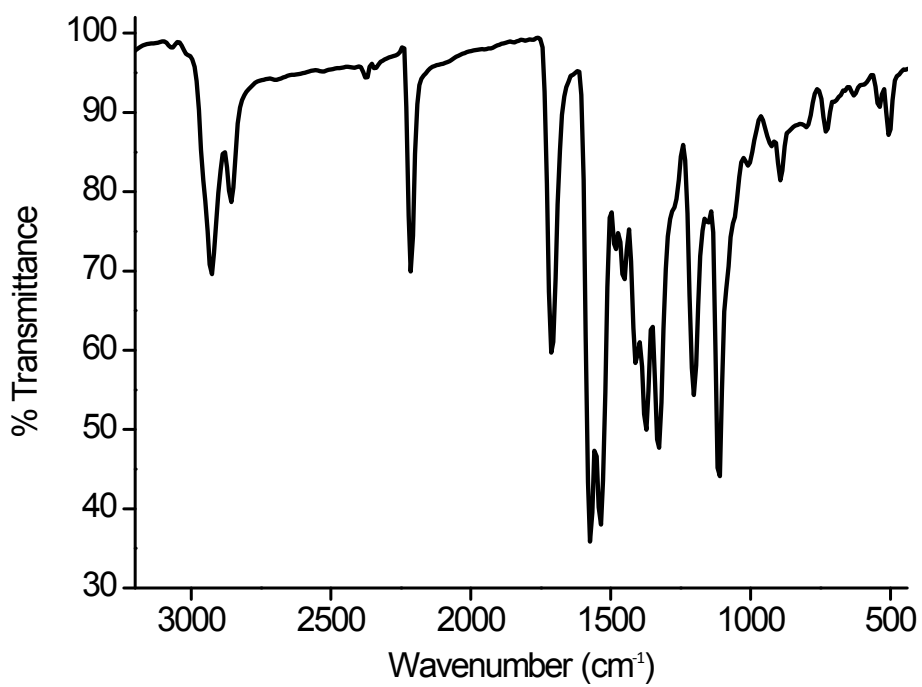


**Figure S14.** FT-IR (KBr) spectrum of compound **FG3**

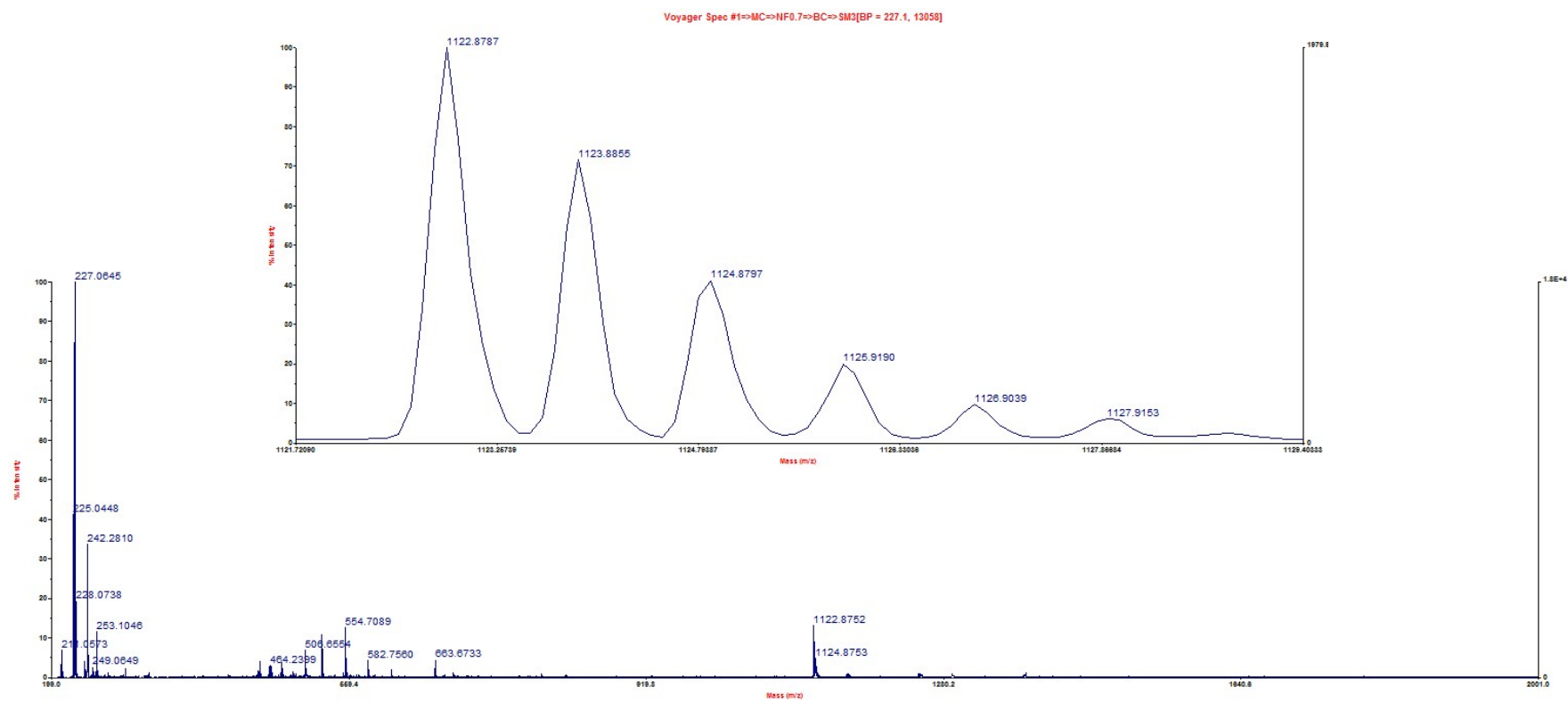


**Figure S15.** MS (MALDI-TOF) spectrum of compound **FG3** (Matrix: Dithranol).

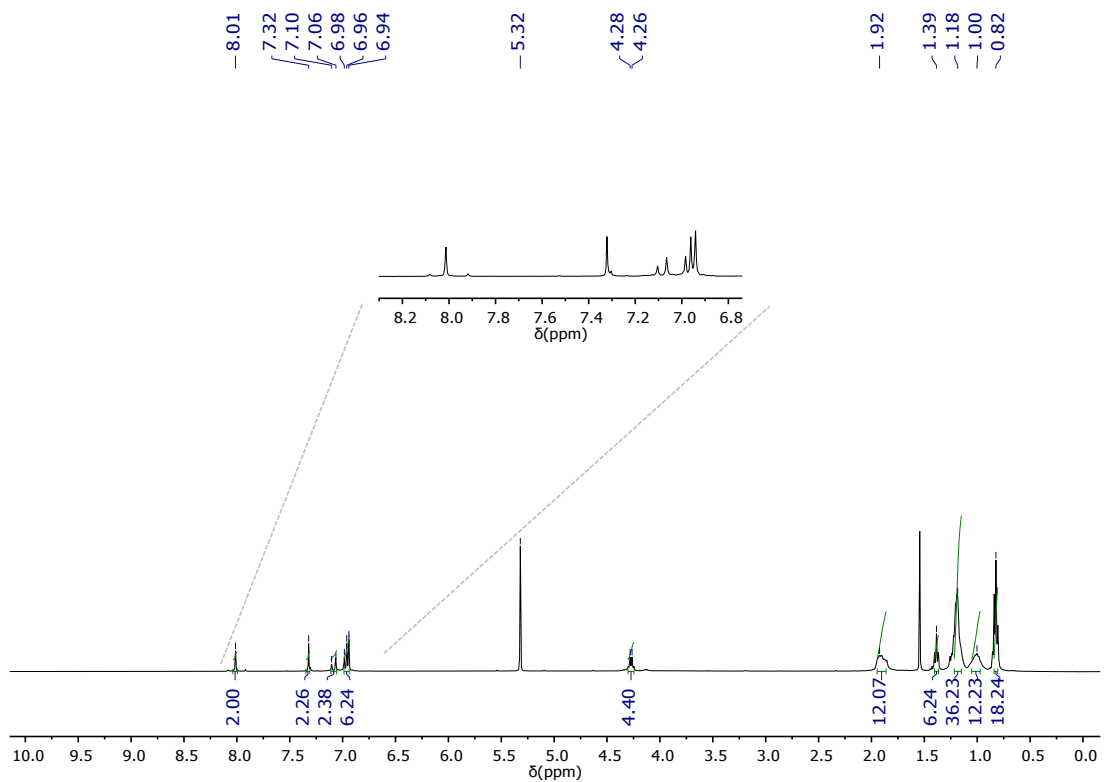


**Figure S16.**  $^1\text{H}$  NMR (400 MHz,  $\text{CD}_2\text{Cl}_2$ ) spectrum of compound **FG4**

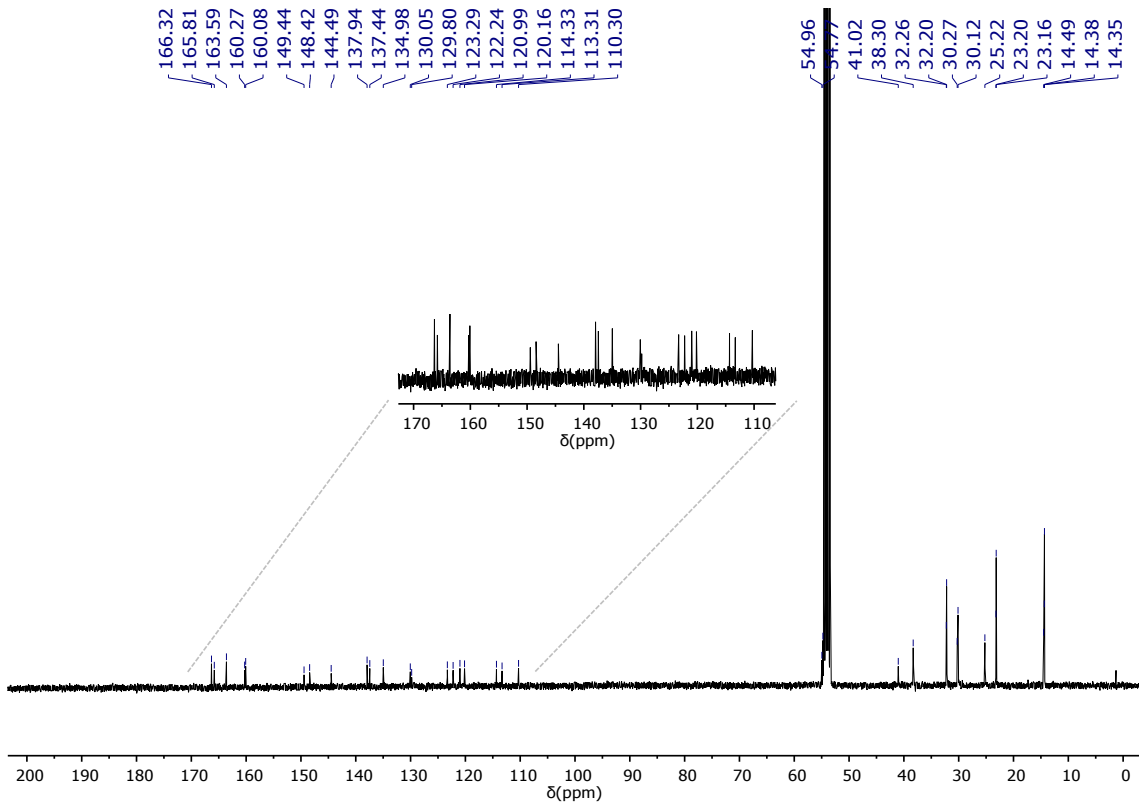
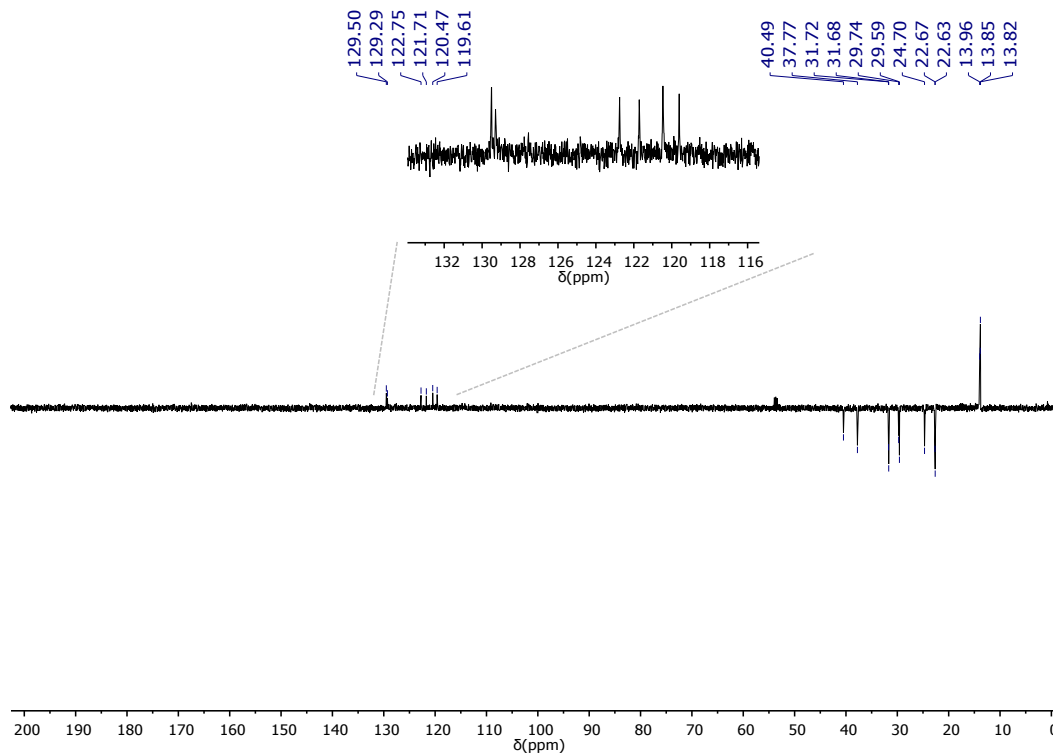
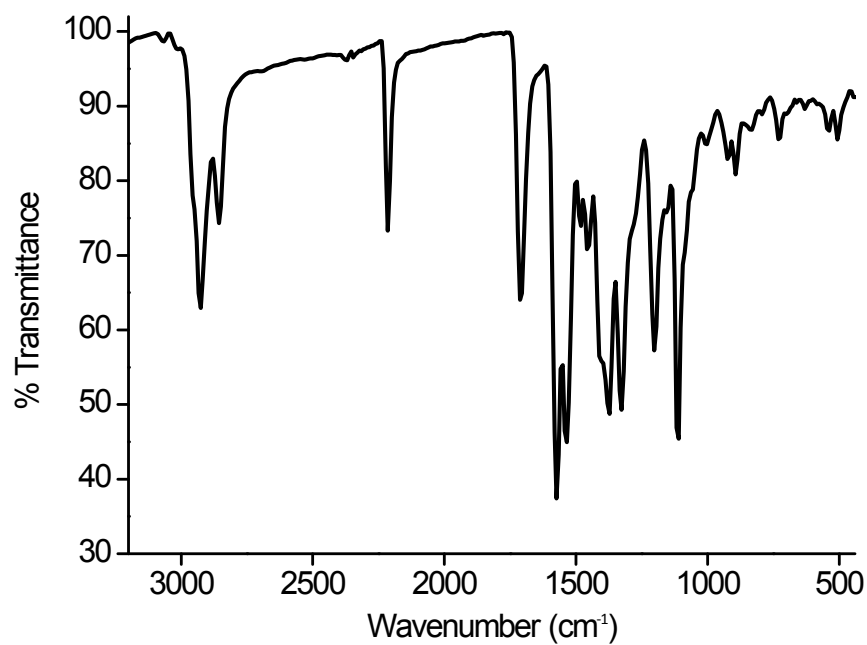


**Figure S17.**  $^{13}\text{C}$  NMR (100 MHz,  $\text{CD}_2\text{Cl}_2$ ) spectrum of compound **FG4**



**Figur**

e S18.  $^{13}\text{C}$  NMR DEPT135 (100 MHz,  $\text{CD}_2\text{Cl}_2$ ) spectrum of compound **FG4**



**Figu**

re S19. FT-IR (KBr) spectrum of compound **FG4**

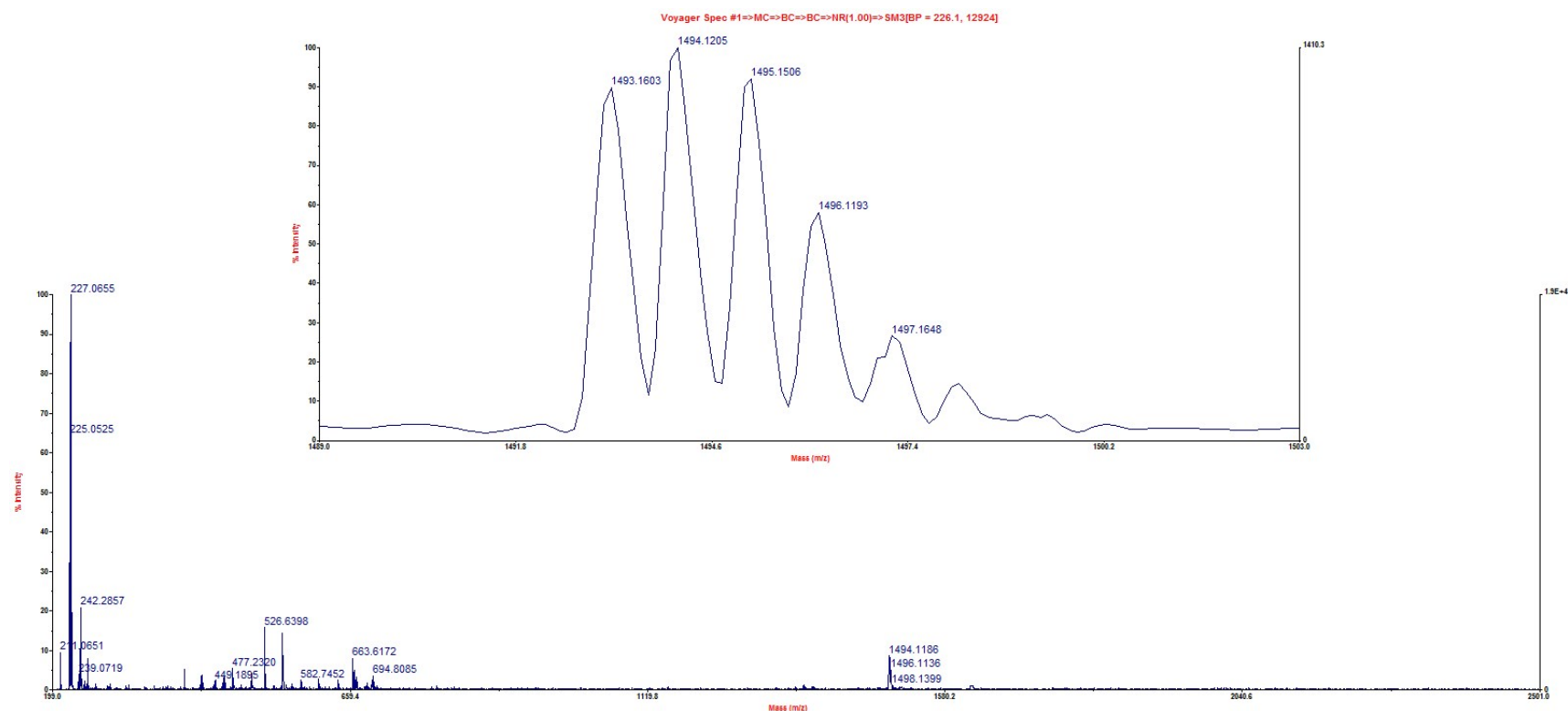


**Figure S20.** MS (MALDI-TOF) spectrum of compound **FG4** (Matrix: Dithranol).

**4. Thermogravimetric Analysis (TGA) and Differential Scanning Calorimetry (DSC) of compounds FG1-4**

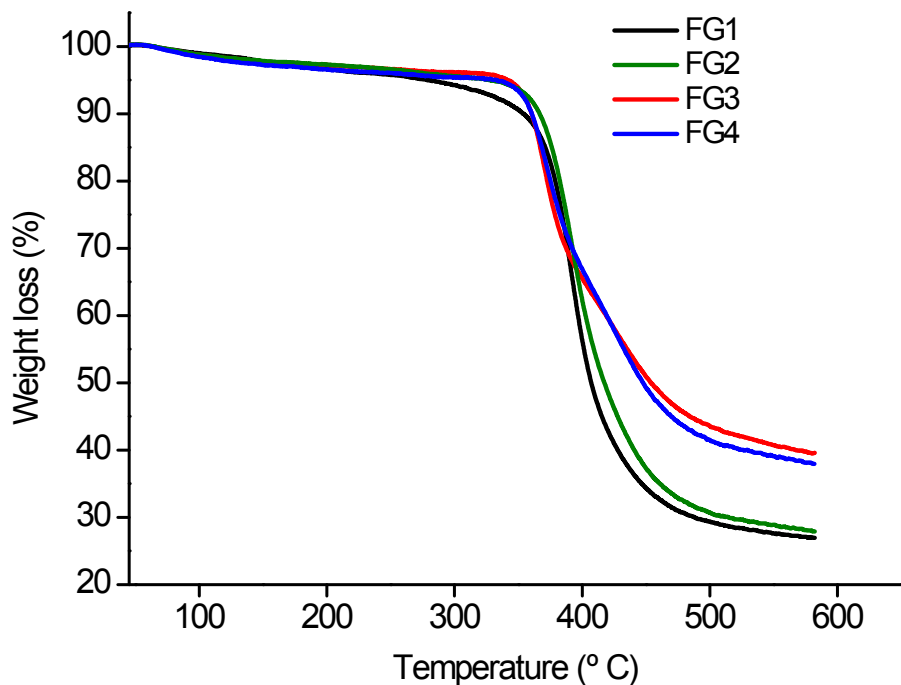


**Figure S21.** TGA curves of oligomers FG1-4 at scan rate of  $10\text{ }^{\circ}\text{C min}^{-1}$

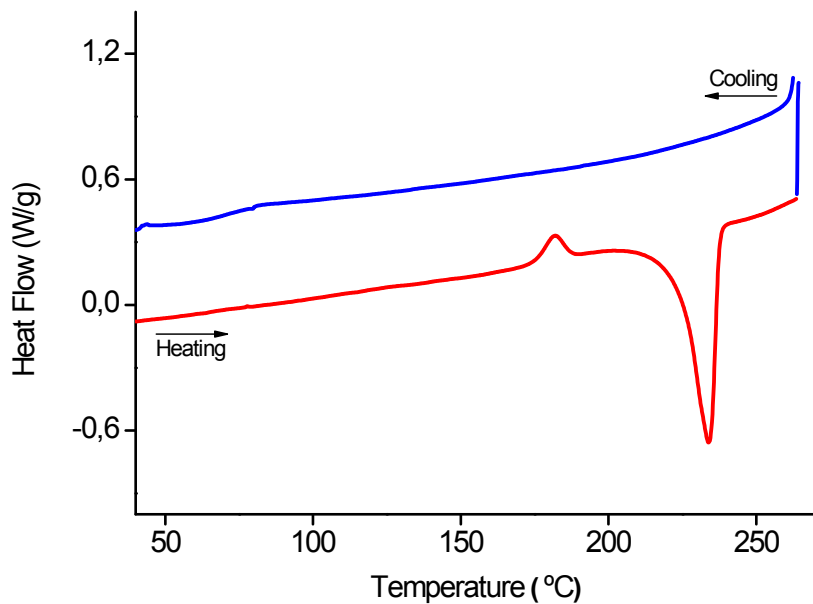


**Figure S22.** DSC curve of compound FG1 at scan rate of  $10\text{ }^{\circ}\text{C min}^{-1}$

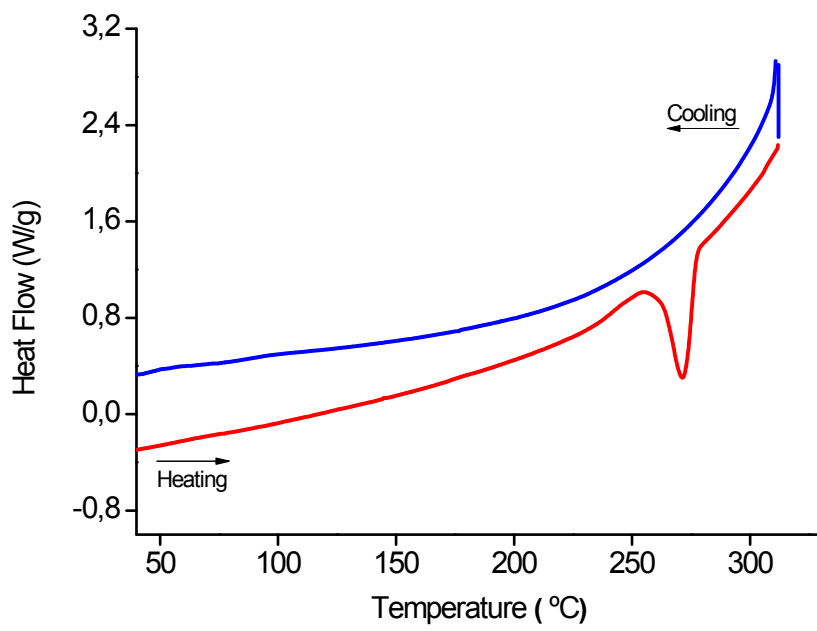


**Figure S23.** DSC curve of compound **FG2** at scan rate of  $10\text{ }^{\circ}\text{C min}^{-1}$

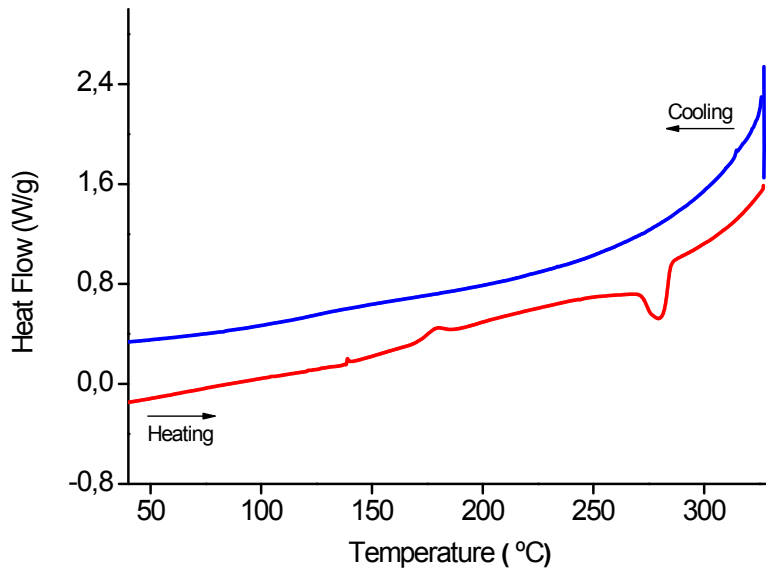


**Figure S24.** DSC curve of compound **FG3** at scan rate of  $10\text{ }^{\circ}\text{C min}^{-1}$

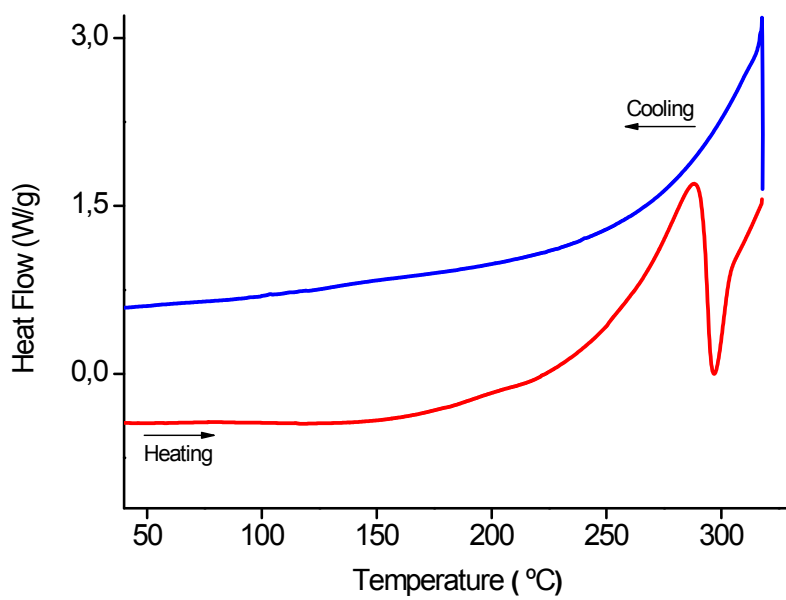


**Figure S25.** DSC curve of compound **FG4** at scan rate of  $10\text{ }^{\circ}\text{C min}^{-1}$

##### 5. Absorption spectrum in solution

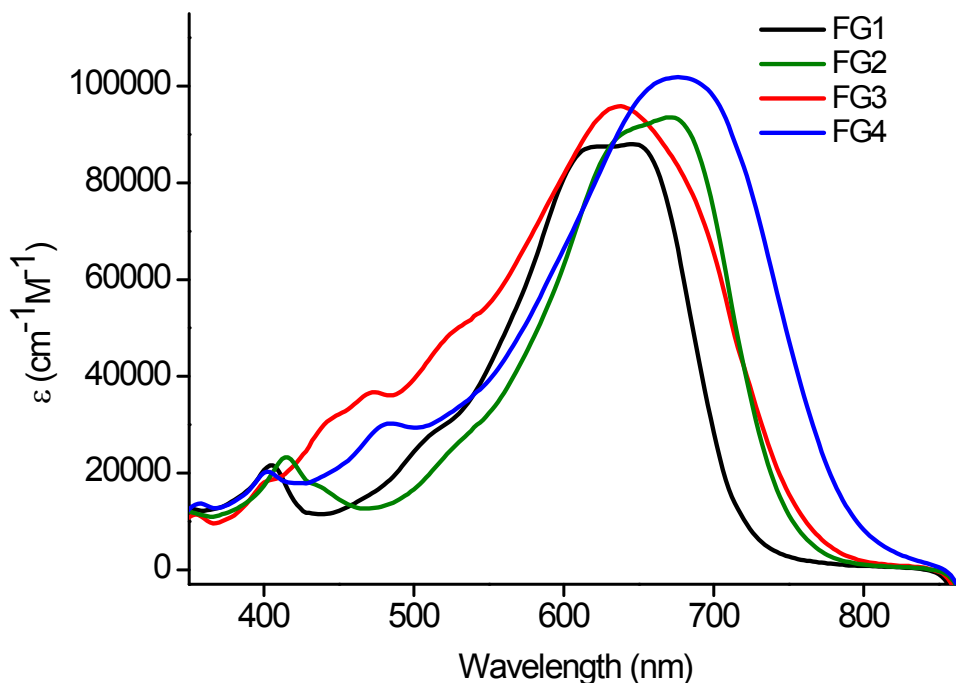


**Figure S26.** UV-Vis absorption spectra in solution for oligomers **FG1-4** (Benzonitrile,  $3 \times 10^{-6}\text{M}$ )

## 6. Electrochemical Studies

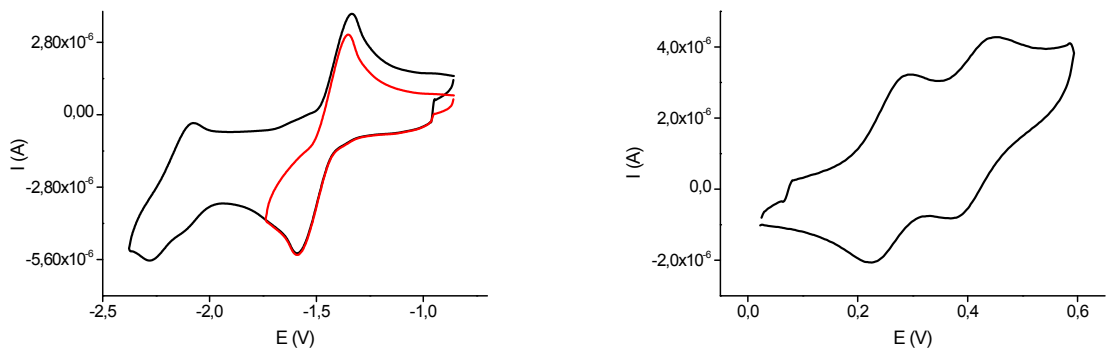


**Figure S27.** Cyclic Voltammetry for oligomer **FG1**

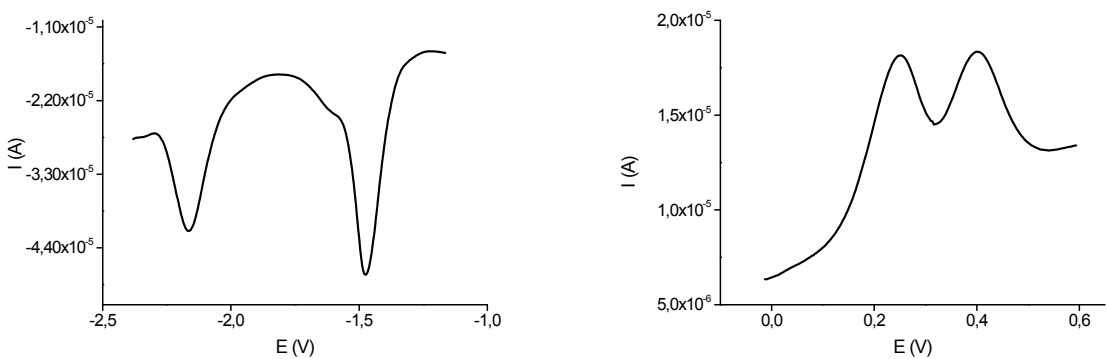


**Figure S28.** Oyster-Young Square Wave Voltammetry for oligomer **FG1**

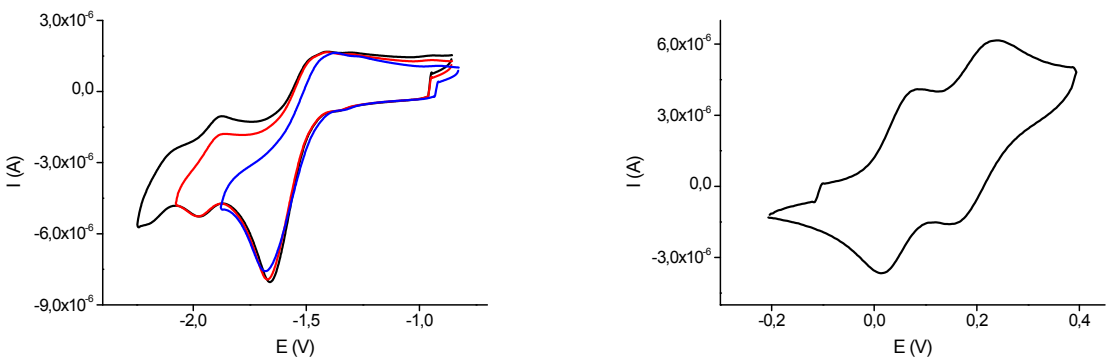


**Figure S29.** Cyclic Voltammetry for oligomer **FG2**

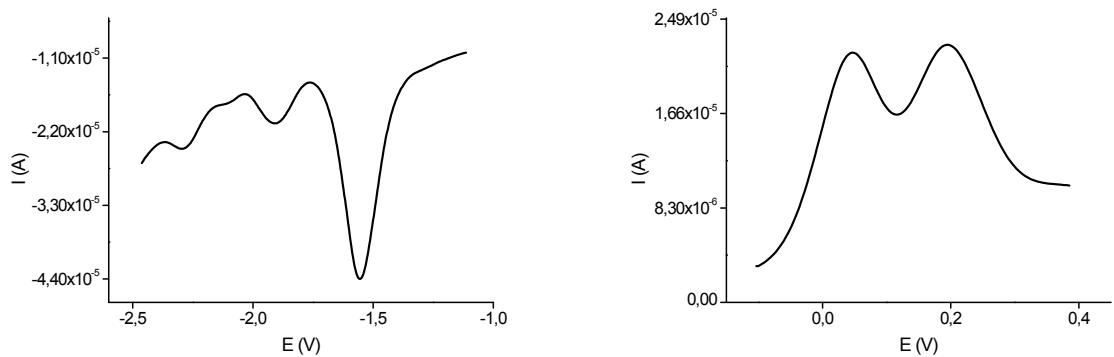


**Figure S30.** Oyster-Young Square Wave Voltammetry for oligomer **FG2**

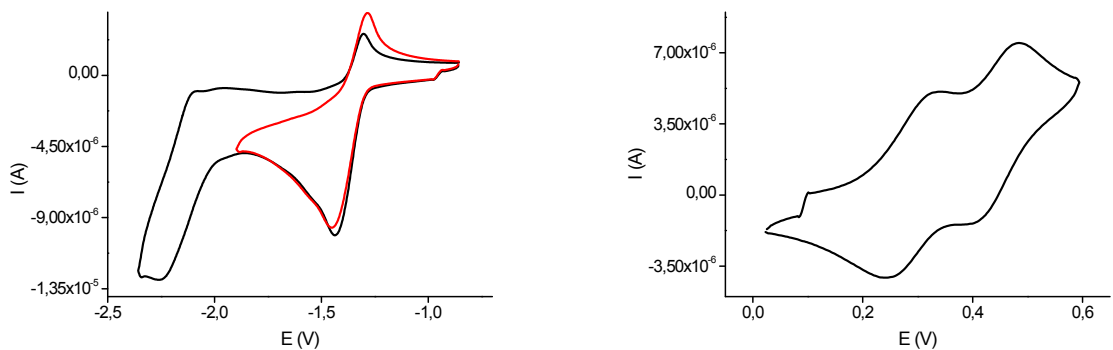


**Figure S31.** Cyclic Voltammetry for oligomer **FG3**

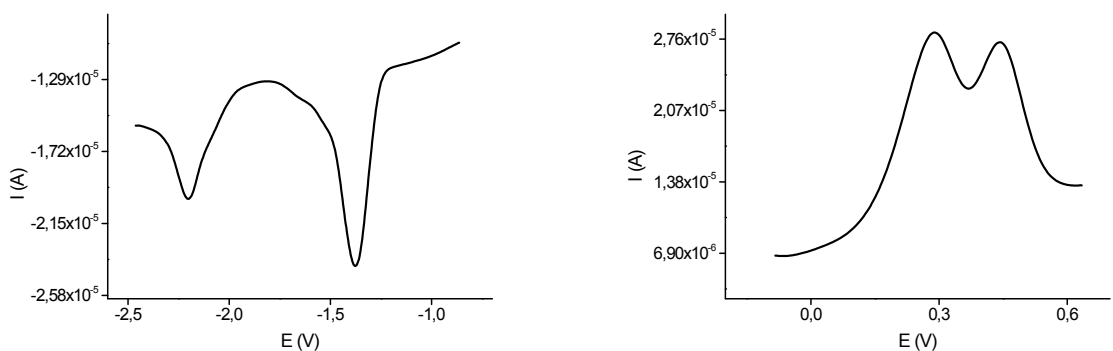


**Figure S32.** Oyster-Young Square Wave Voltammetry for oligomer **FG3**

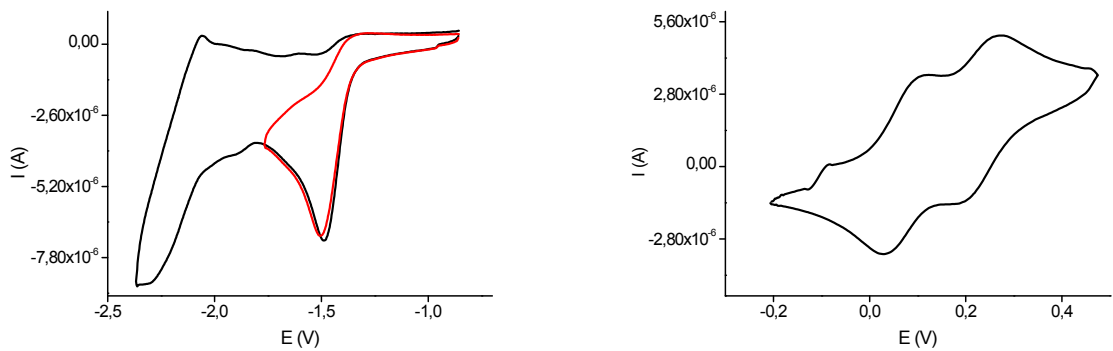


**Figure S33.** Cyclic Voltammetry for oligomer **FG4**

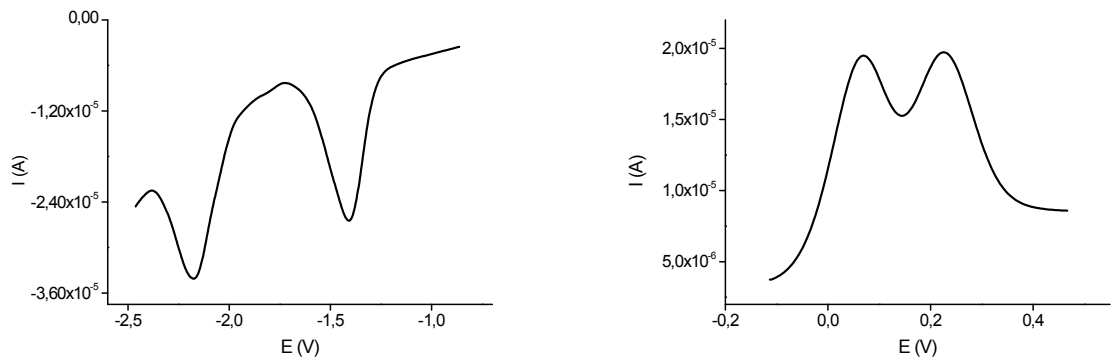


**Figure S34.** Oyster-Young Square Wave Voltammetry for oligomer **FG4**

## 7. Theoretical calculations

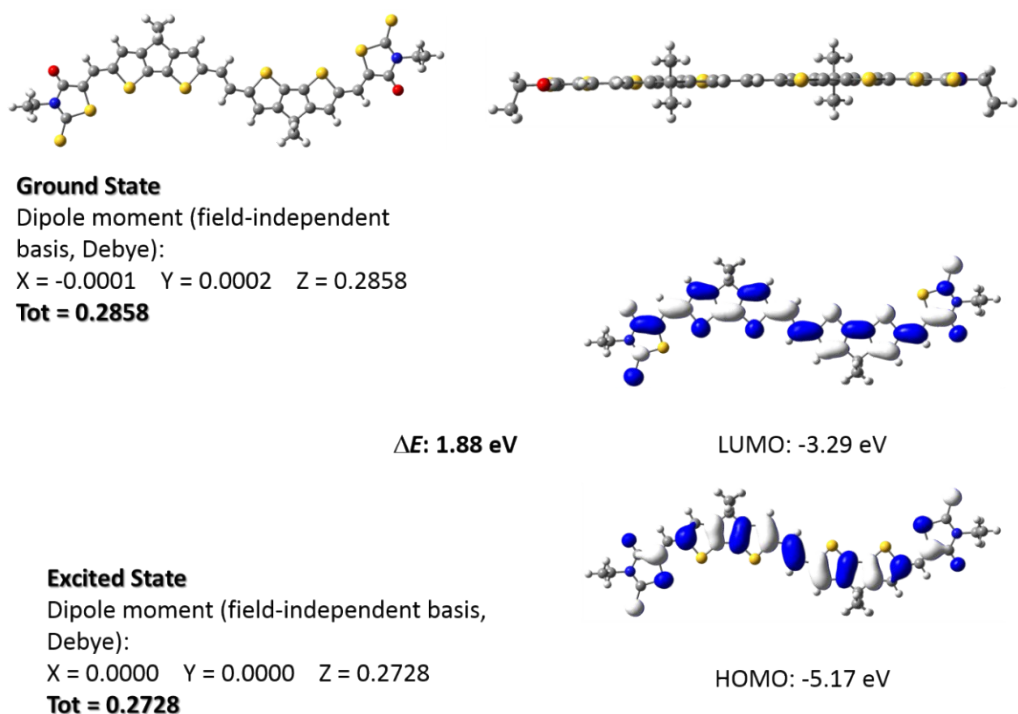


**Figure S35.** Optimized geometry, dipole moment and HOMO and LUMO electron density distribution for oligomer **FG1**

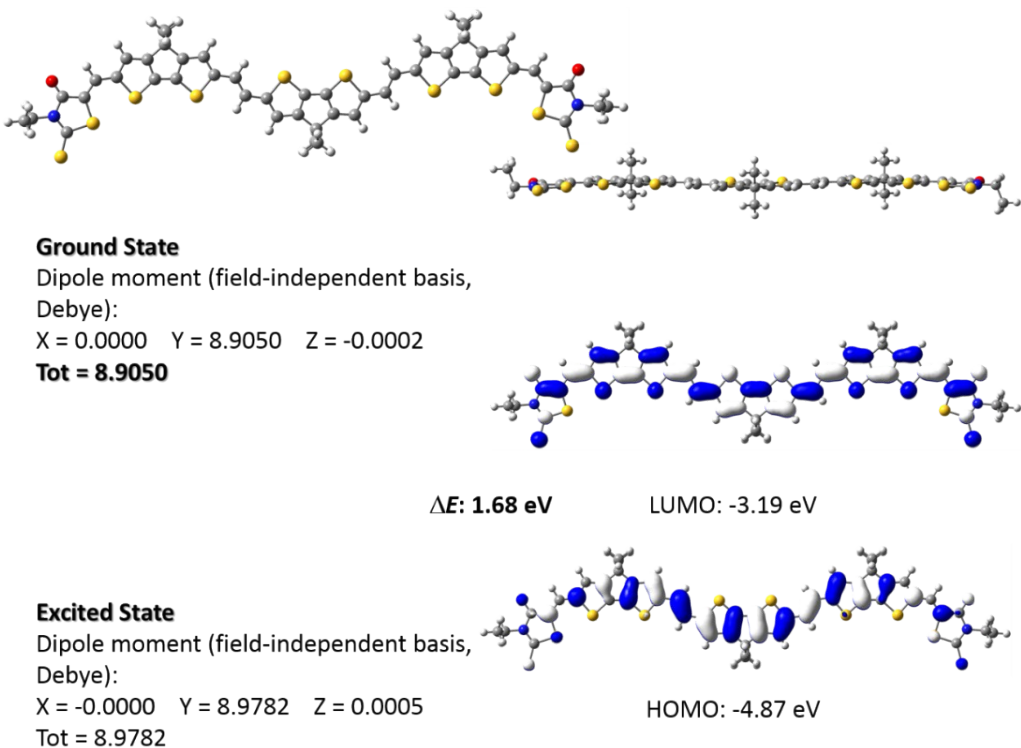


**Figure S36.** Optimized geometry, dipole moment and HOMO and LUMO electron density distribution for oligomer **FG2**

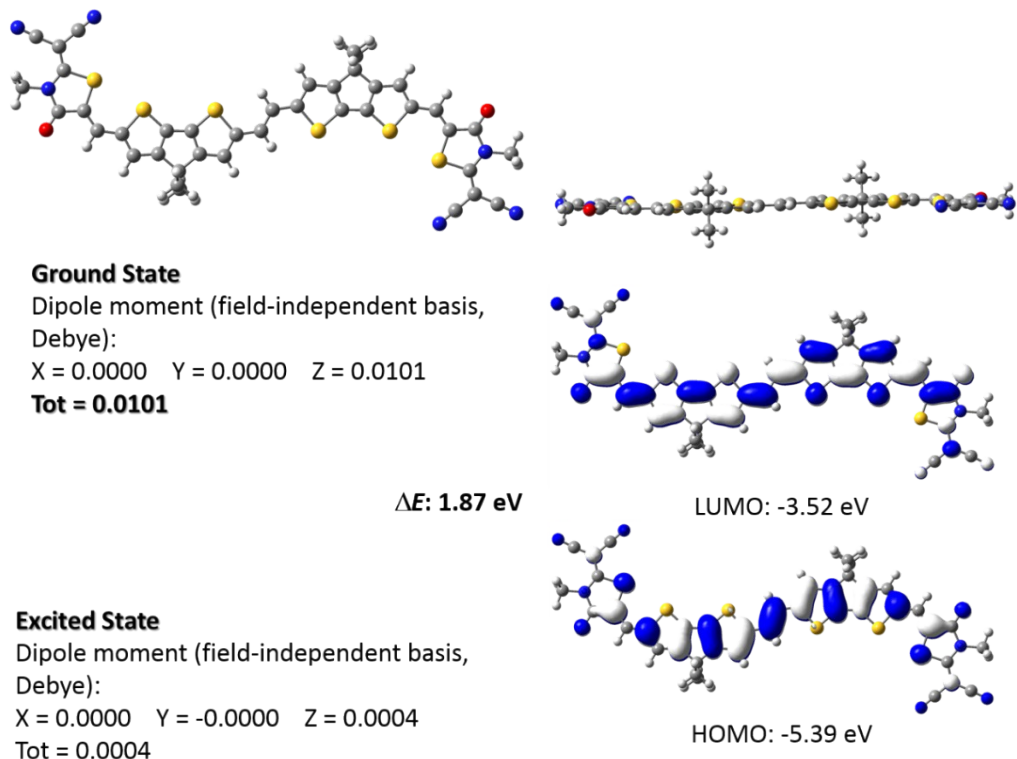


**Figure S37.** Optimized geometry, dipole moment and HOMO and LUMO electron density distribution for oligomer **FG3**

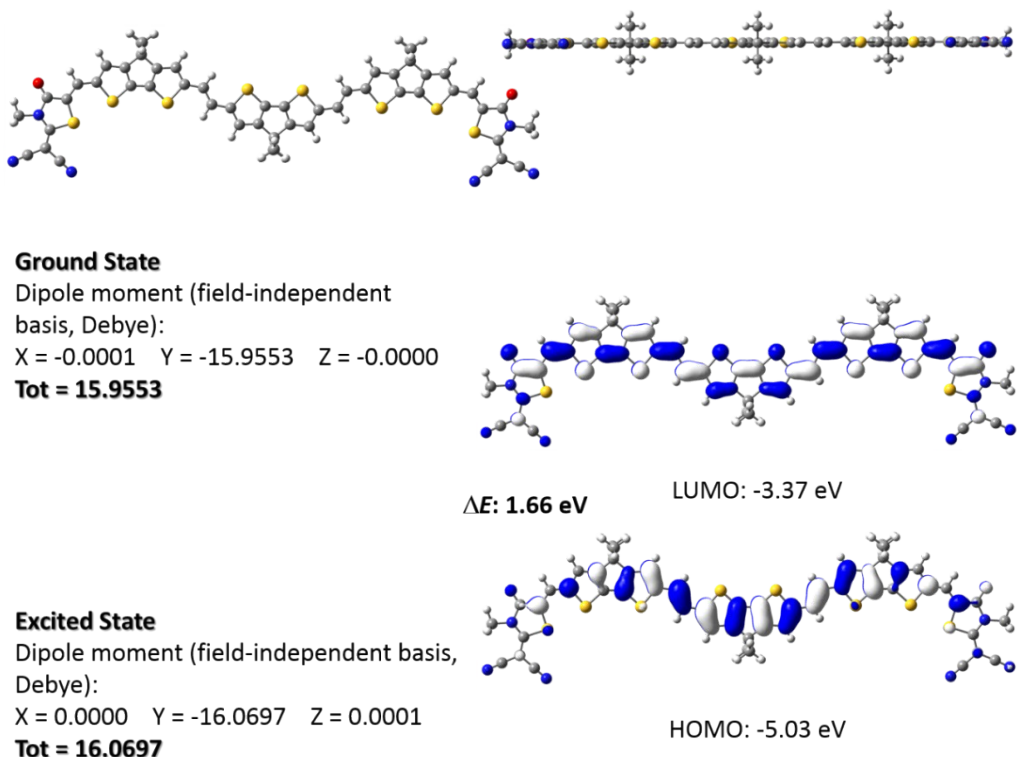


**Figure S38.** Optimized geometry, dipole moment and HOMO and LUMO electron density distribution for oligomer **FG4**

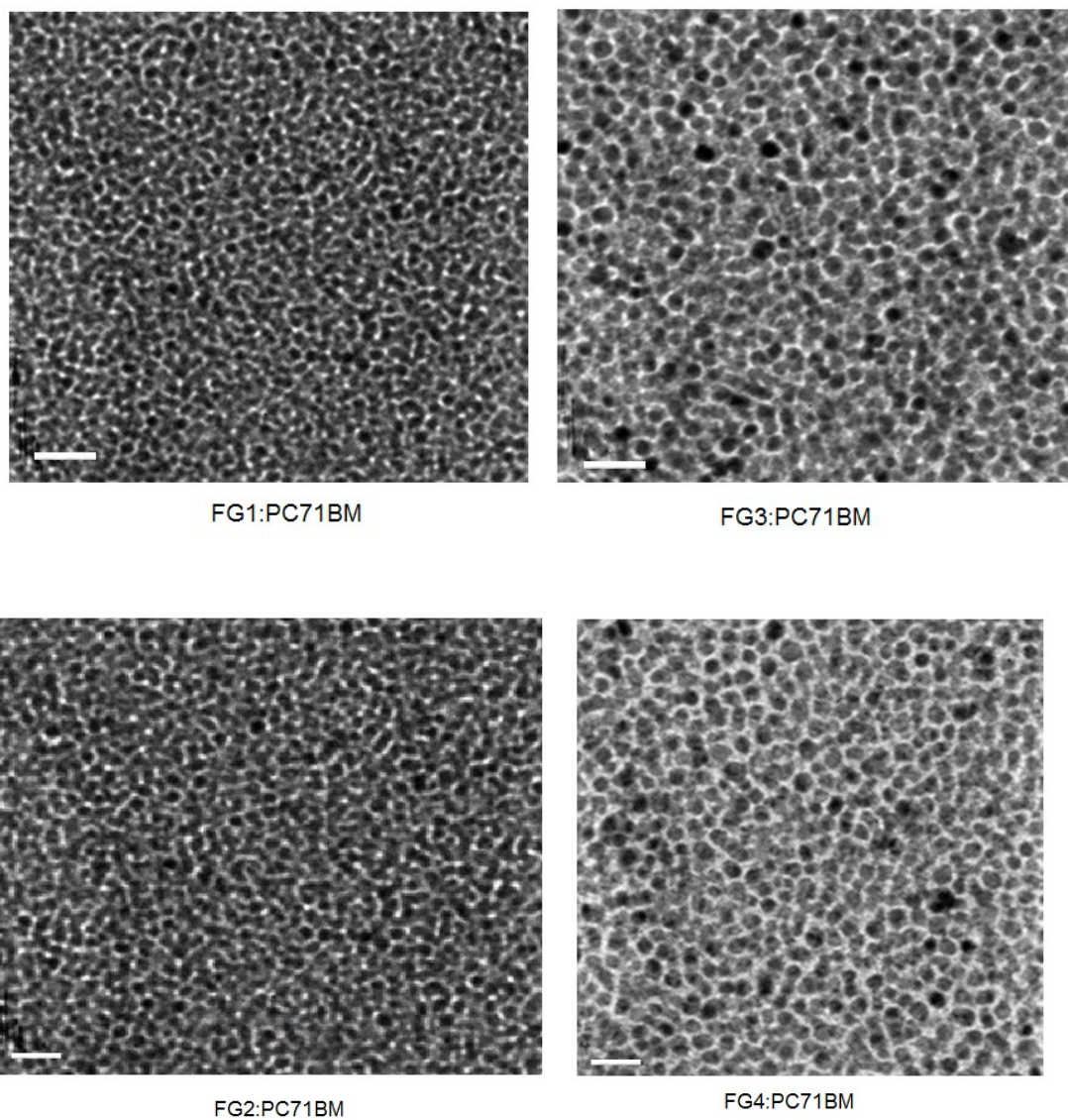


**Figure S39.** TEM images of the optimized **FG1:PC<sub>71</sub>BM**, **FG2:PC<sub>71</sub>BM**, **FG3:PC<sub>71</sub>BM** and **FG4:PC<sub>71</sub>BM** active layers, scale bar is 200 nm.